Electronic Supplementary Information for:

A sustainable strategy for the assembly of Glypromate® and its structurally-related analogues by tandem sequential peptide coupling

Ivo E. Sampaio-Dias,[†,a] Luís Pinto da Silva,[b,c] Sandra G. Silva,[a]

Xerardo García-Mera,[d] and José E. Rodríguez-Borges[a]

[a.] LAQV/REQUIMTE, *Department of Chemistry and Biochemistry, Faculty of Sciences, University of Porto, R. Campo Alegre 697, 4169-007 Porto, Portugal.*

[b.] *Chemistry Research Unit (CIQUP), Department of Chemistry and Biochemistry, Faculty of Sciences, University of Porto, R. Campo Alegre 697, 4169-007 Porto, Portugal.*

[c.] *LACOMEPHI, GreenUPorto, Department of Geosciences, Environment and Territorial Planning, Faculty of Sciences, University of Porto, R. Campo Alegre 697, 4169-007 Porto, Portugal.*

[d.] *Department of Organic Chemistry, Faculty of Pharmacy, University of Santiago de Compostela, E-15782 Santiago de Compostela, Spain*

† **Corresponding author e-mail**:
idias@fc.up.pt (Ivo E. Sampaio-Dias)

Electronic Supplementary Information

Table of contents

1. NMR spectra for peptides **5**, **7-11** and **13** and PyBOP-NHS interaction ESI-2
2. rp-HPLC chromatogram for tripeptide **5** ESI-16
3. VT-NMR and *in silico* study for the *cis-trans* isomerization of tripeptide **5** ESI-16
4. E-factor calculation for tripeptide **5** ESI-22
5. Cartesian coordinates for *cis* and *trans*-**5** ESI-24

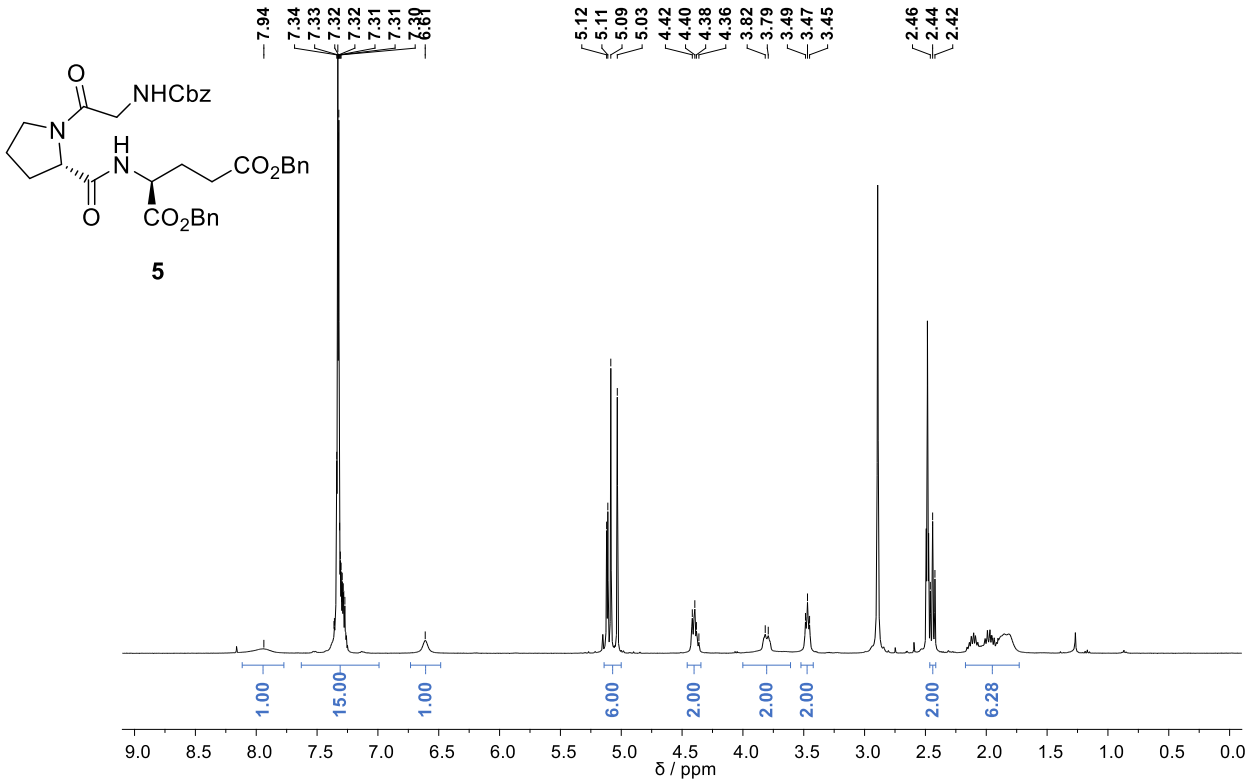

Figure S1. ^{1}H-NMR spectrum (400 MHz, DMSO-d_6, 110 ºC) of compound **5**.

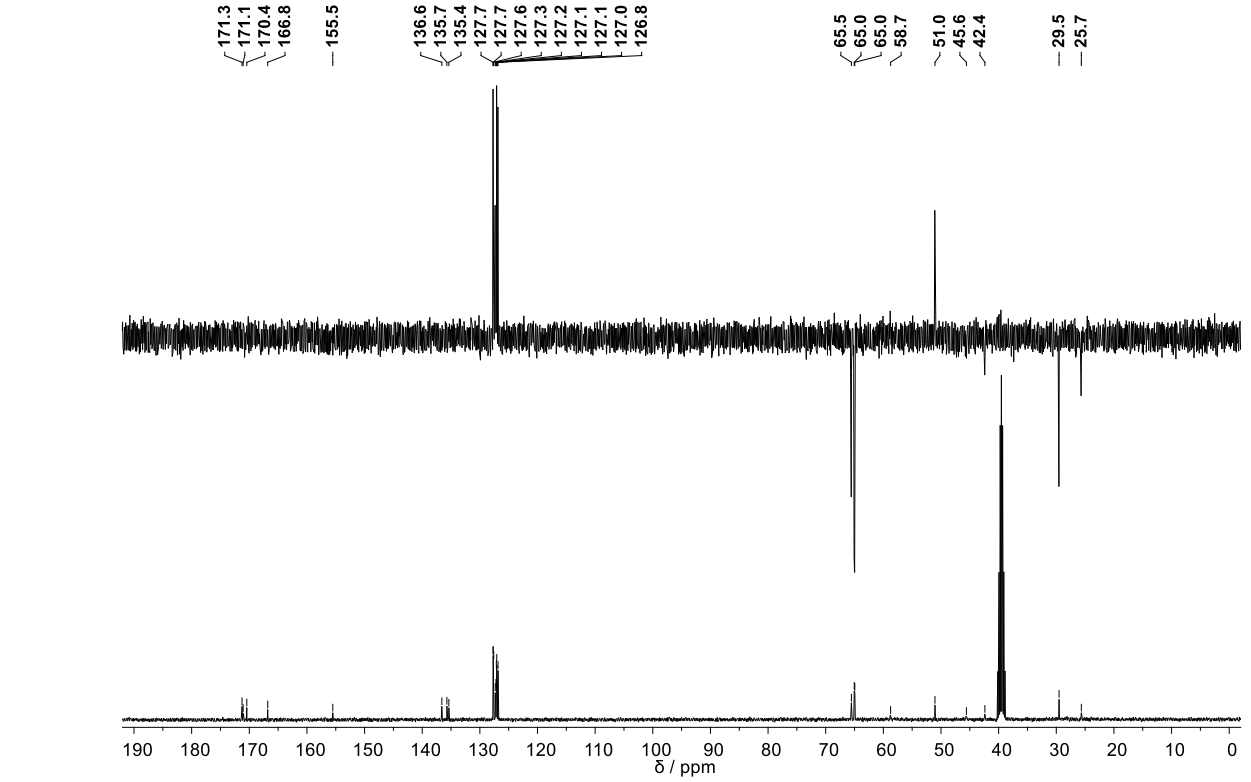

Figure S2. ^{13}C-NMR and DEPT-135 spectra (100 MHz, DMSO-d_6, 110 ºC) of compound **5**.

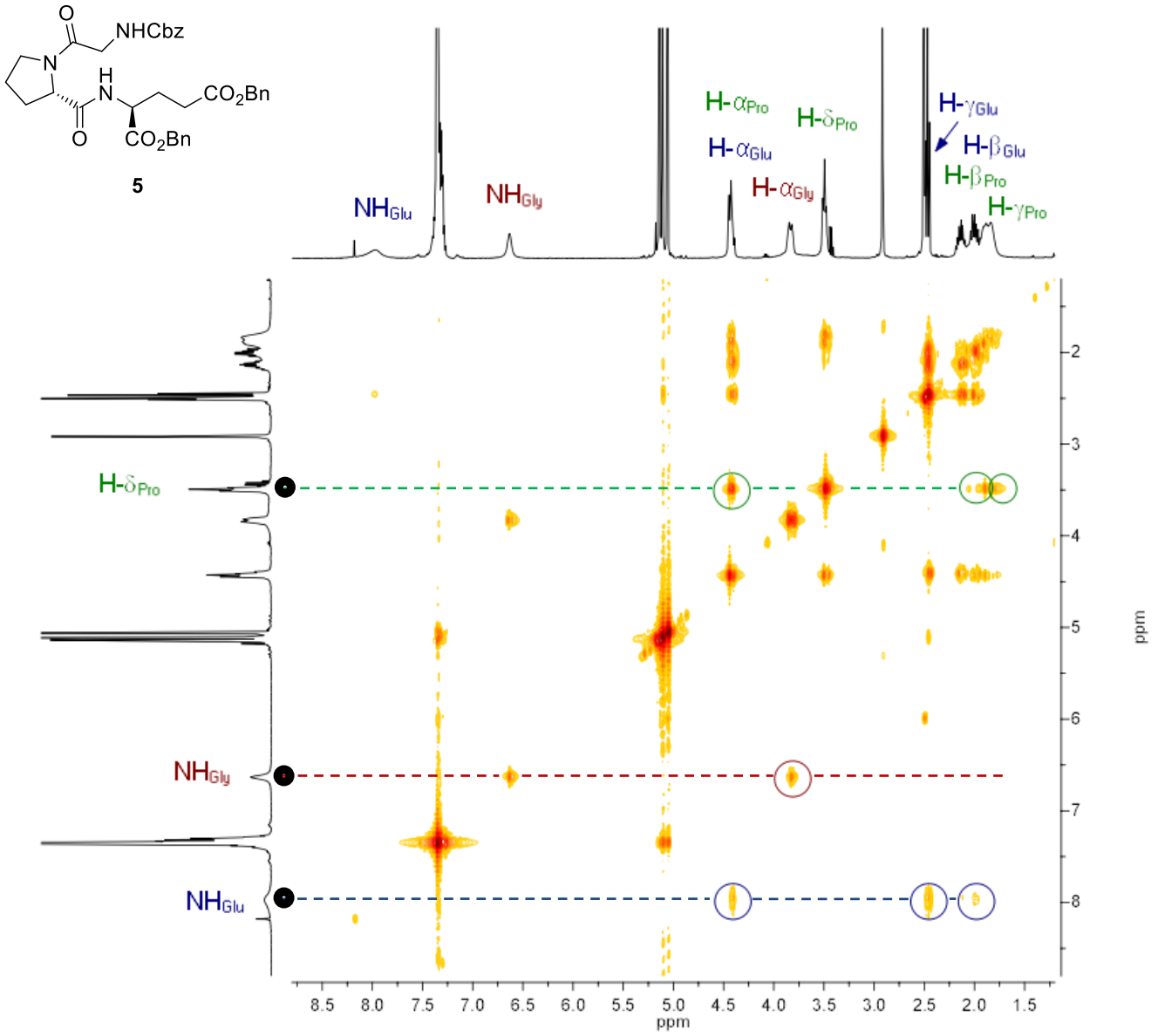

Figure S3. TOCSY spectrum (400 MHz, DMSO-d_6, 110 ºC) of compound **5**.

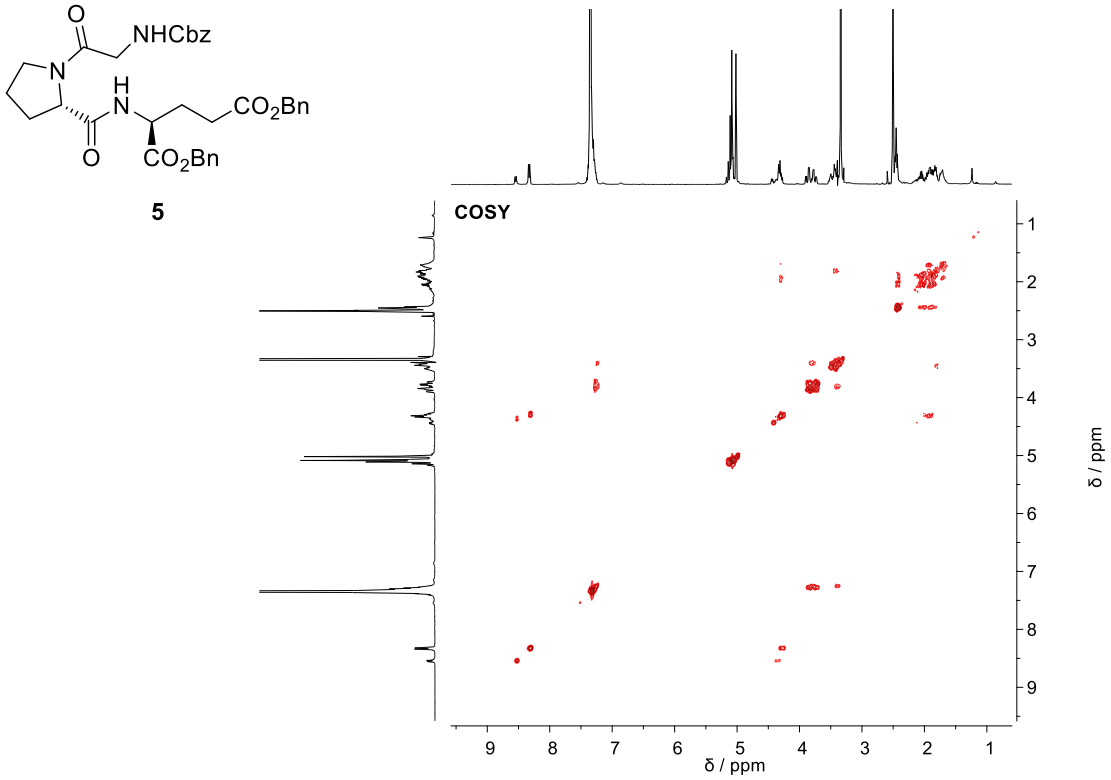

Figure S4. COSY spectrum (400 MHz, DMSO-d_6, 26 ºC) of **5**.

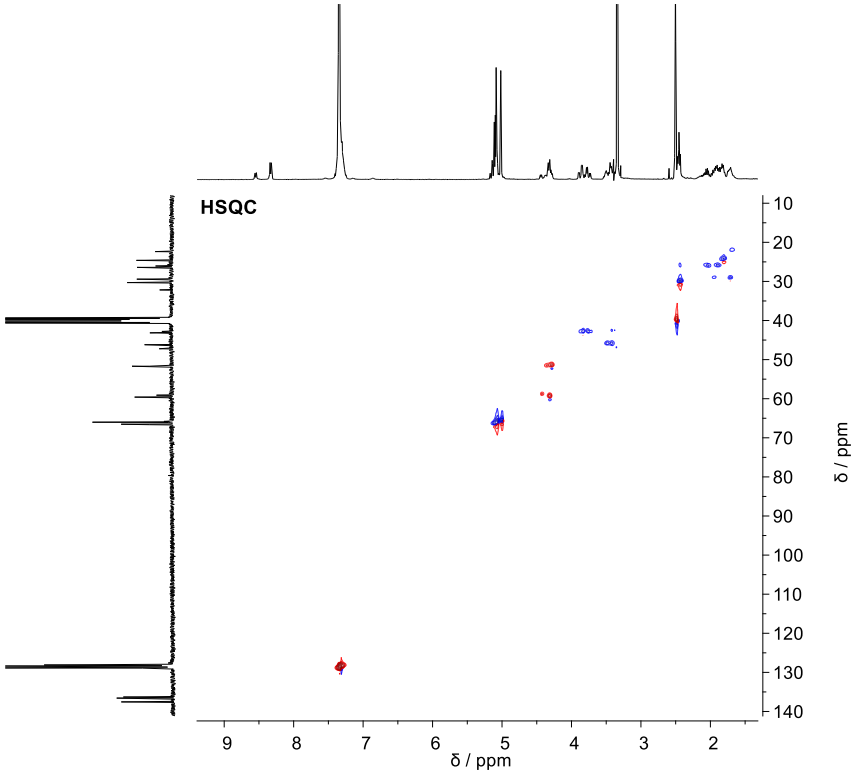

Figure S5. HSQC spectrum (400 MHz, DMSO-d_6, 26 ºC) of **5**.

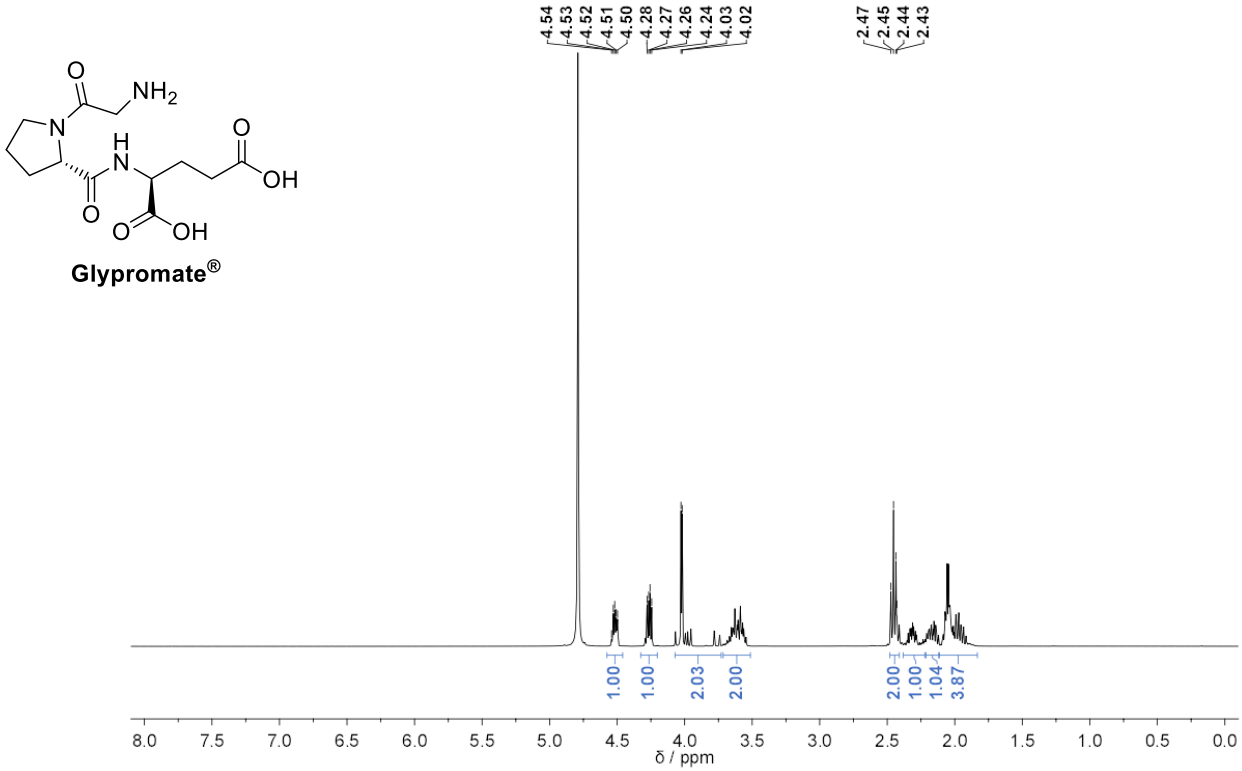

Figure S6. ^{1}H-NMR spectrum (400 MHz, D_2O, 26 ºC) of Glypromate®.

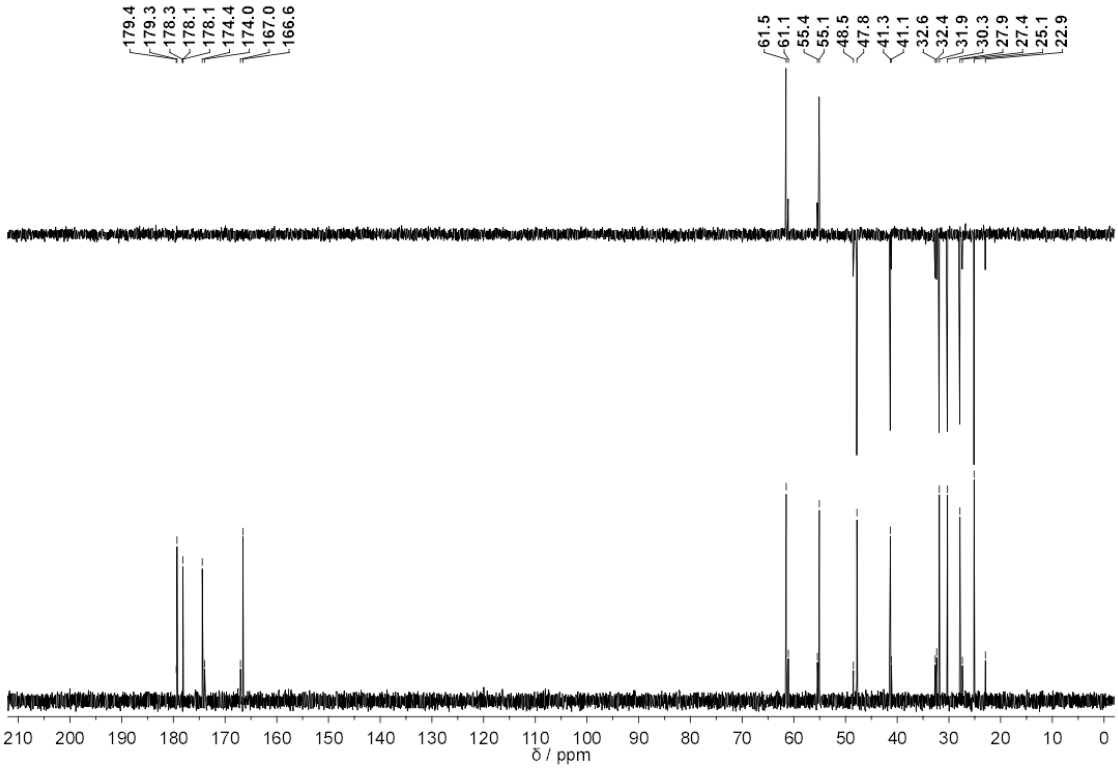

Figure S7. ^{13}C-NMR and DEPT-135 spectra (100 MHz, D_2O, 26 ºC) of Glypromate®.

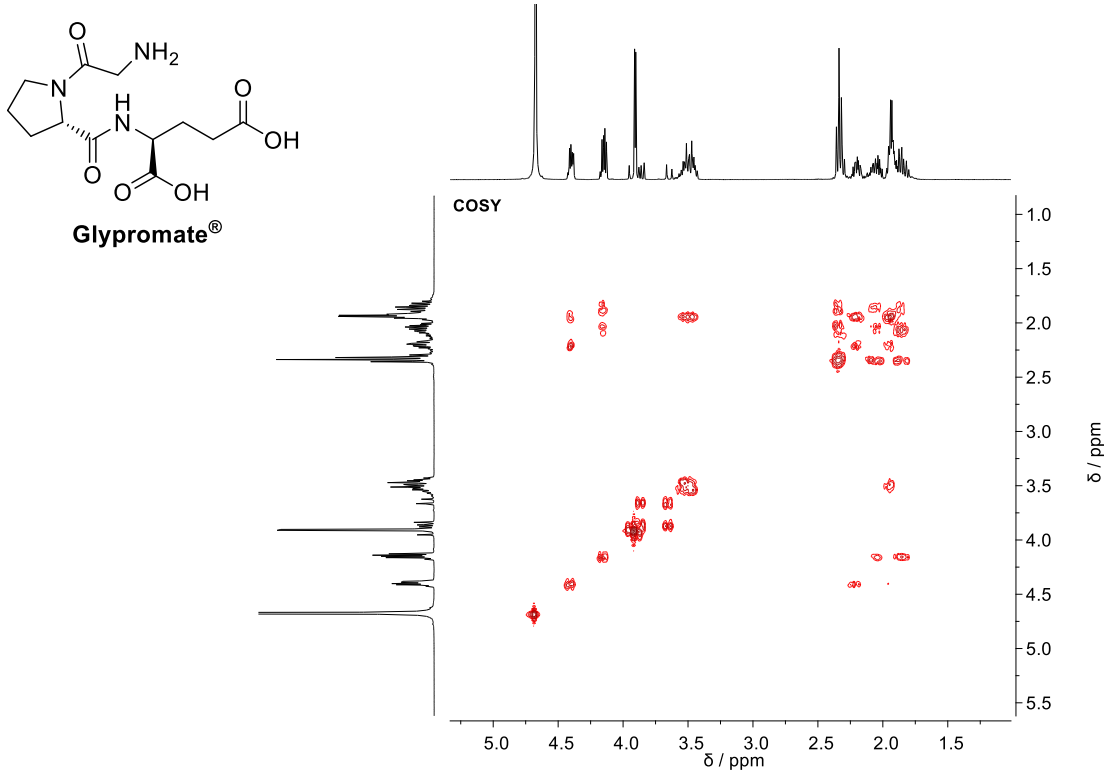

Figure S8. COSY spectrum (400 MHz, D_2O, 26 ºC) of Glypromate®.

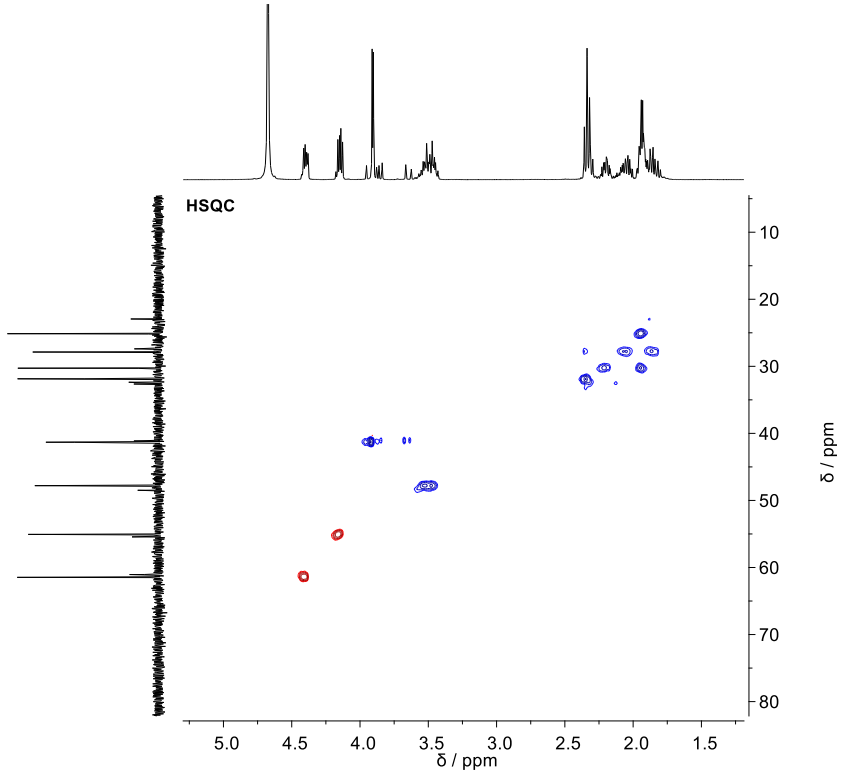

Figure S9. HSQC spectrum (400 MHz, D_2O, 26 ºC) of Glypromate®.

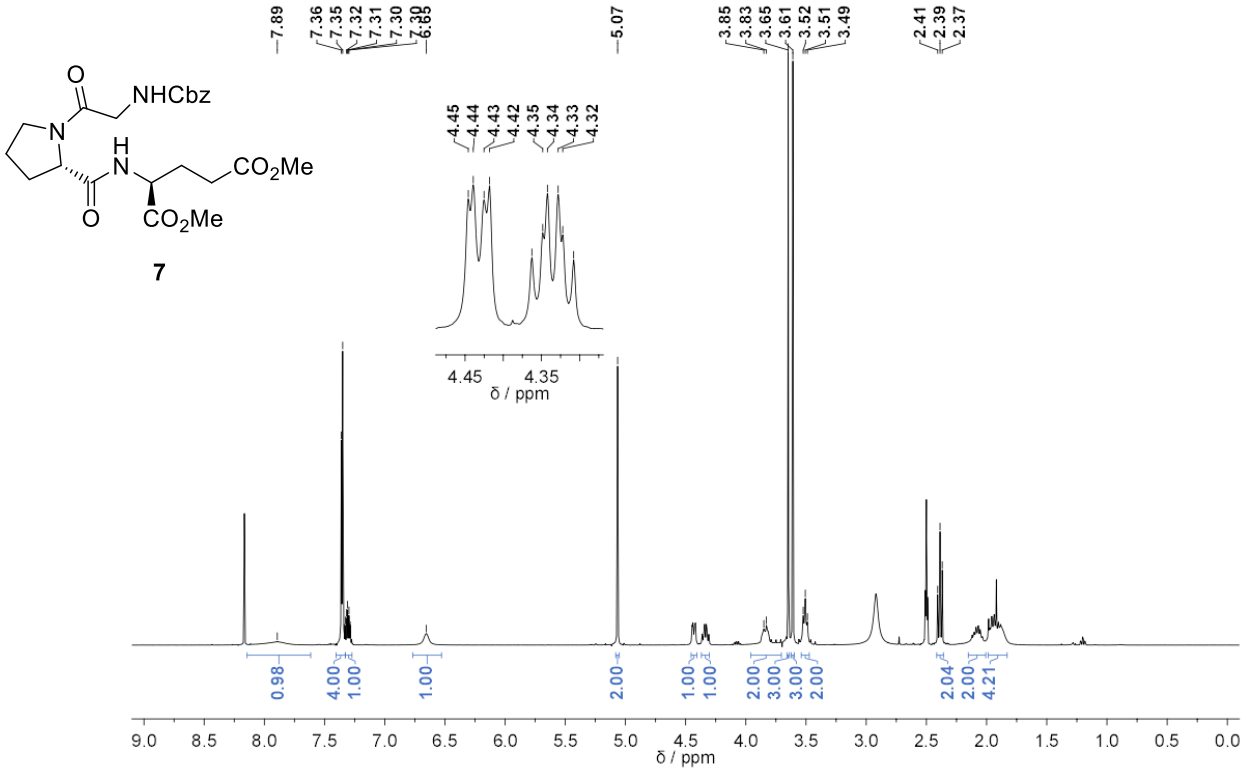

Figure S10. ^{1}H-NMR spectrum (400 MHz, DMSO-d_6, 110 ºC) of compound **7**.

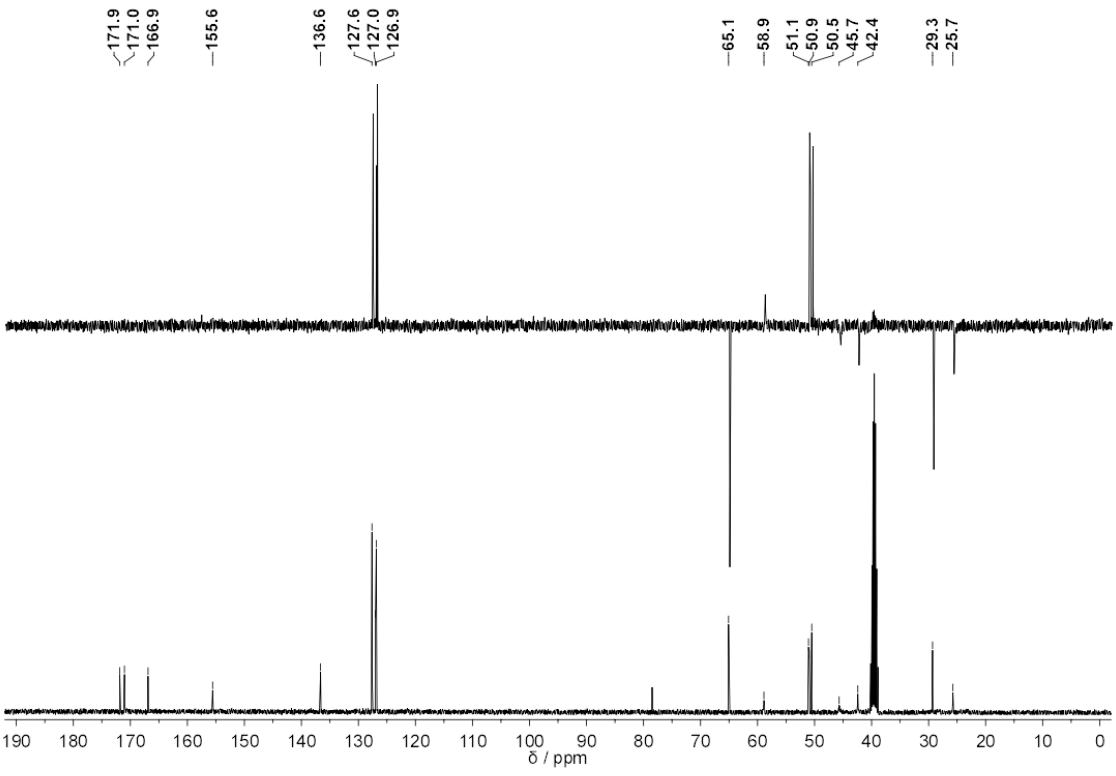

Figure S11. ^{13}C-NMR and DEPT-135 spectra (100 MHz, DMSO-d_6, 110 ºC) of compound **7**.

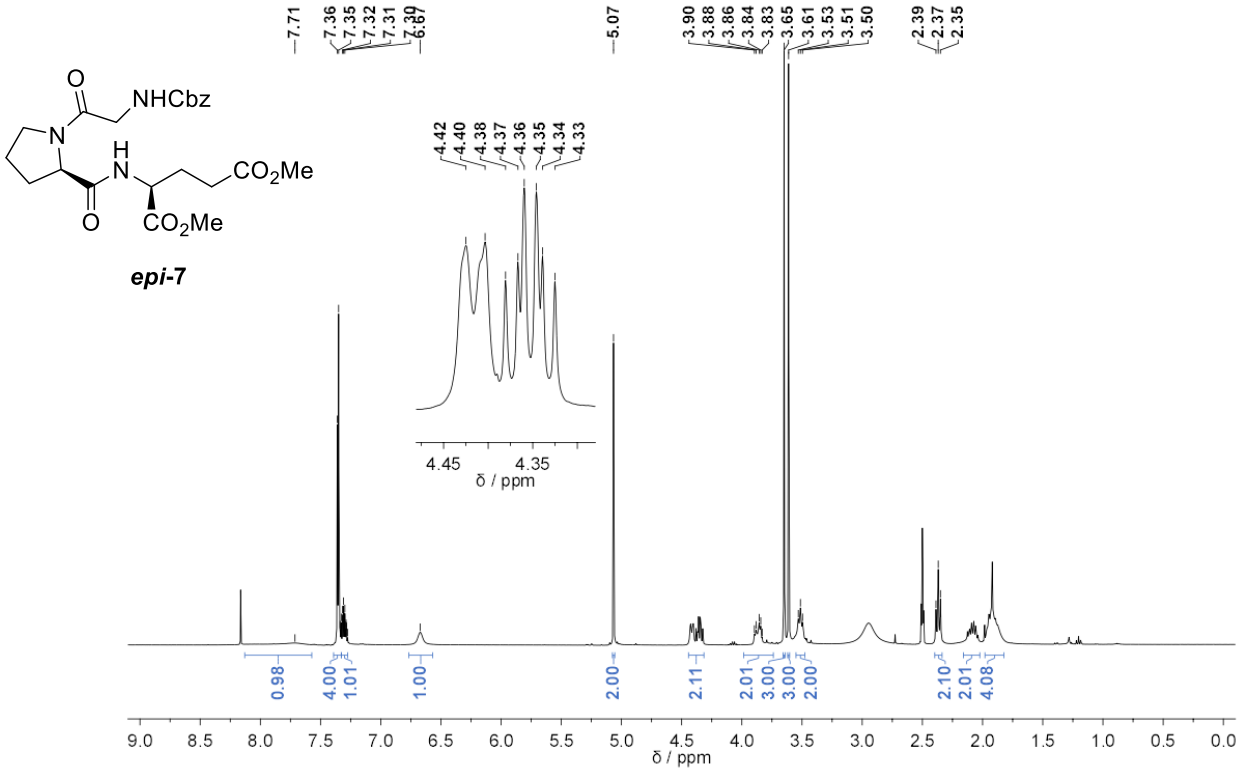

Figure S12. ^{1}H-NMR spectrum (400 MHz, DMSO-d_6, 110 ºC) of compound ***epi*-7**.

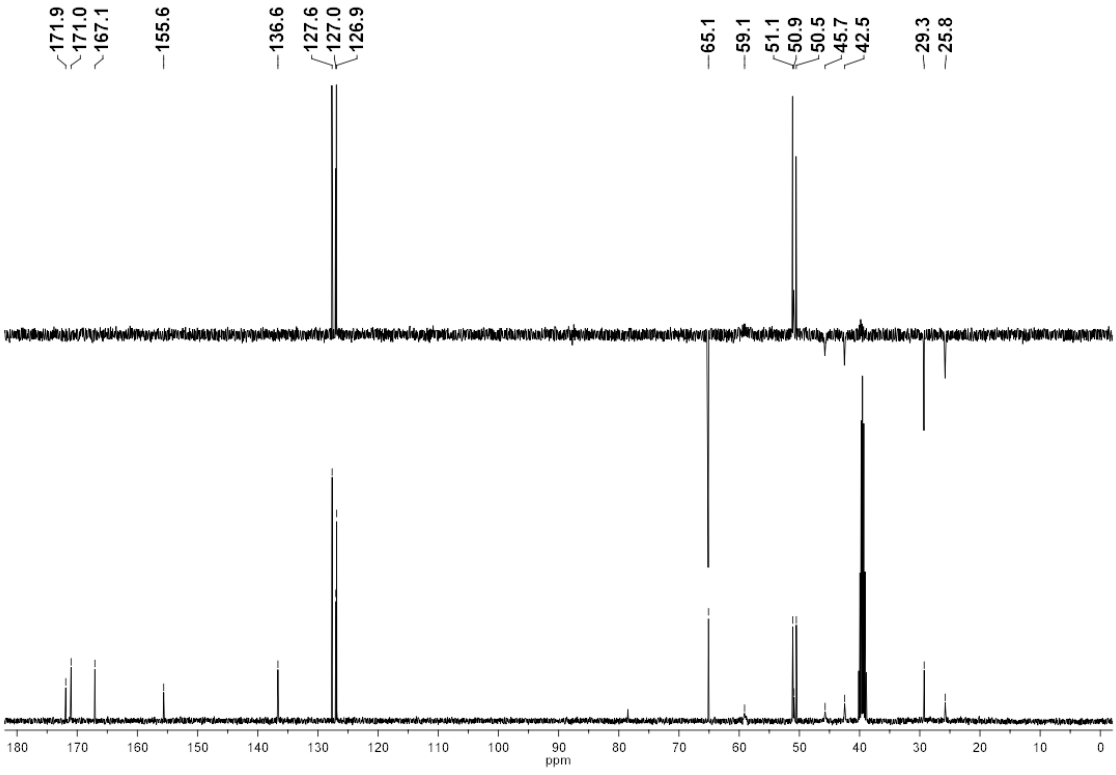

Figure S13. ^{13}C-NMR and DEPT-135 spectra (100 MHz, DMSO-d_6, 110 ºC) of compound ***epi*-7**.

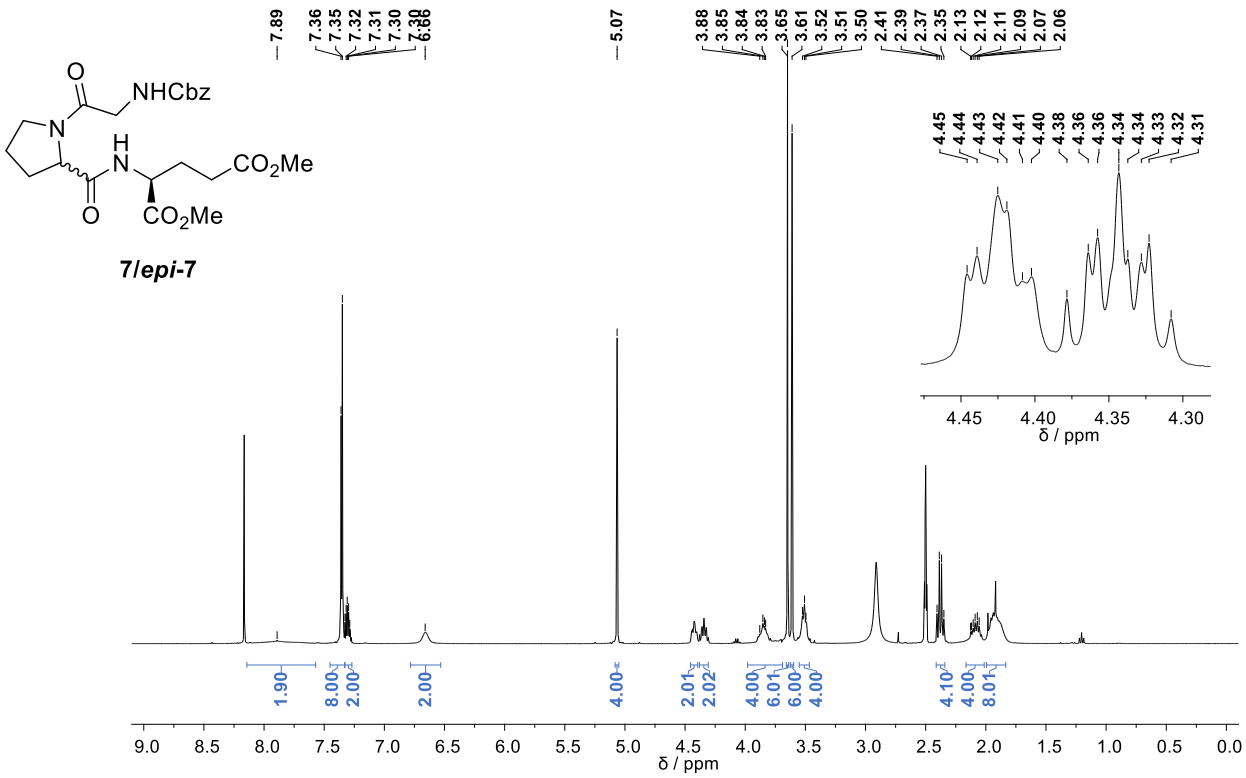

Figure S14. ^{1}H-NMR spectrum (400 MHz, DMSO-d_6, 110 ºC) of compounds **7**/***epi*-7**.

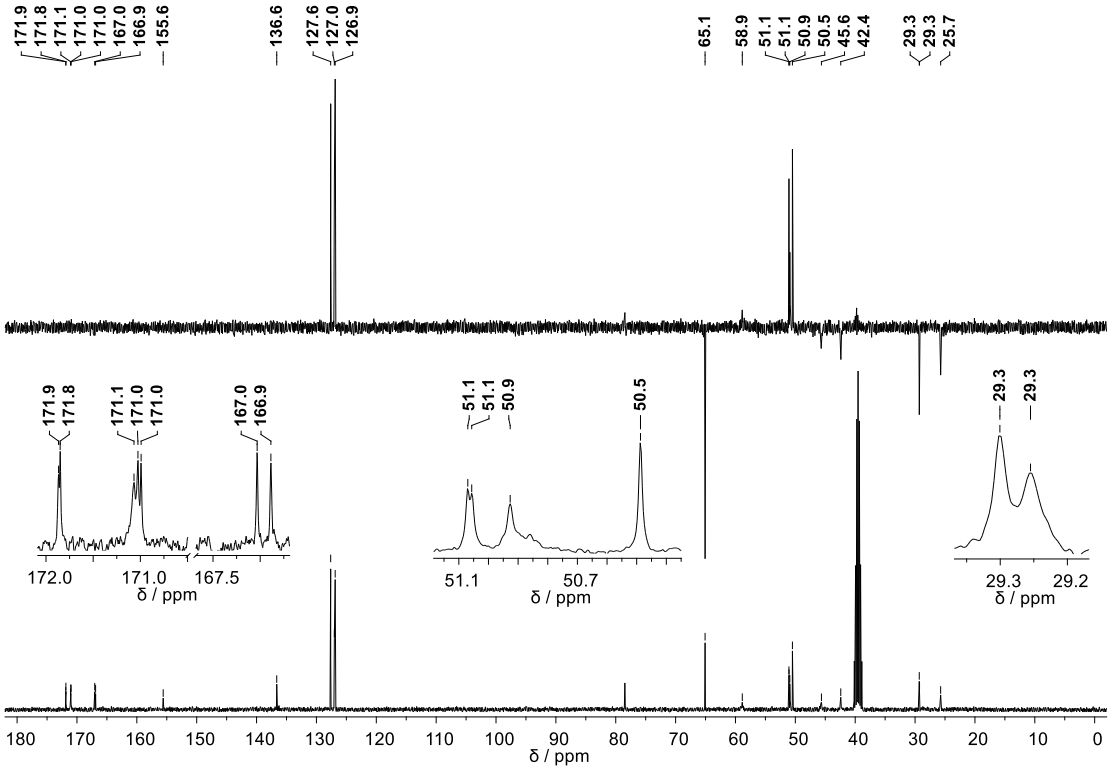

Figure S15. ^{13}C-NMR and DEPT-135 spectra (100 MHz, DMSO-d_6, 110 ºC) of compounds **7**/***epi*-7**.

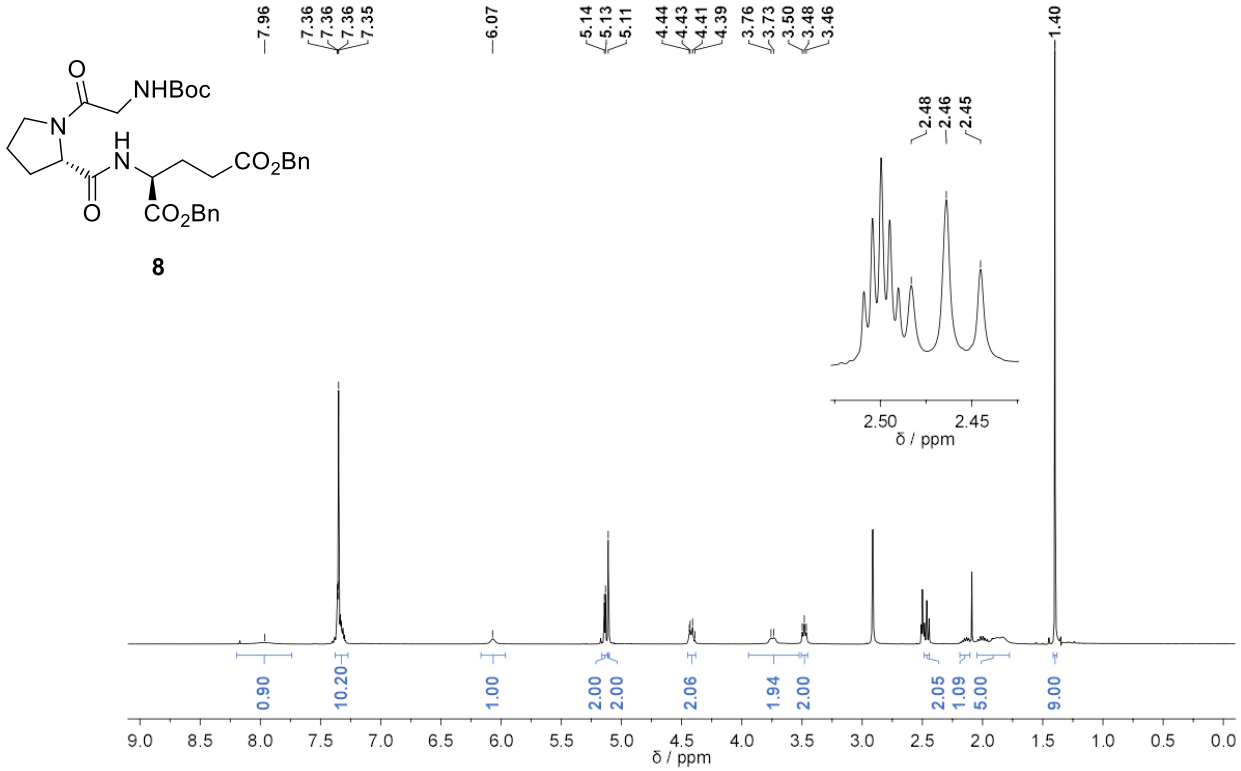

Figure S16. ^{1}H-NMR spectrum (400 MHz, DMSO-d_6, 110 ºC) of compound **8**.

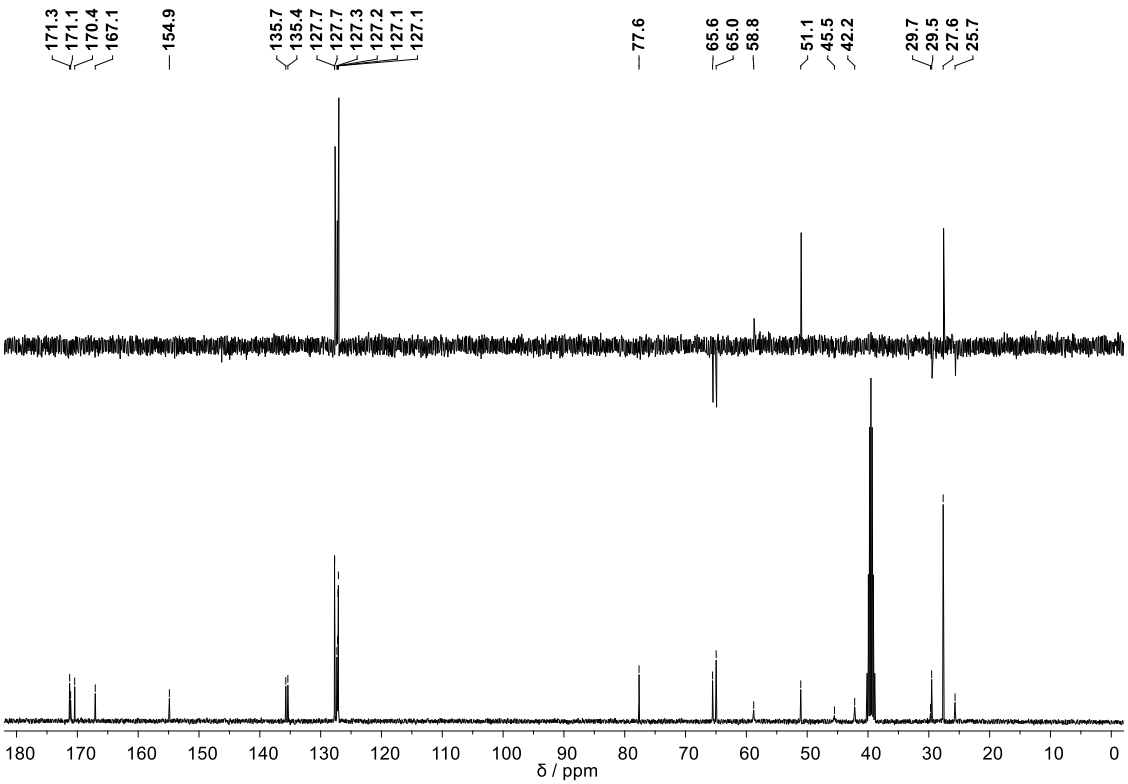

Figure S17. ^{13}C-NMR and DEPT-135 spectra (100 MHz, DMSO-d_6, 110 ºC) of compound **8**.

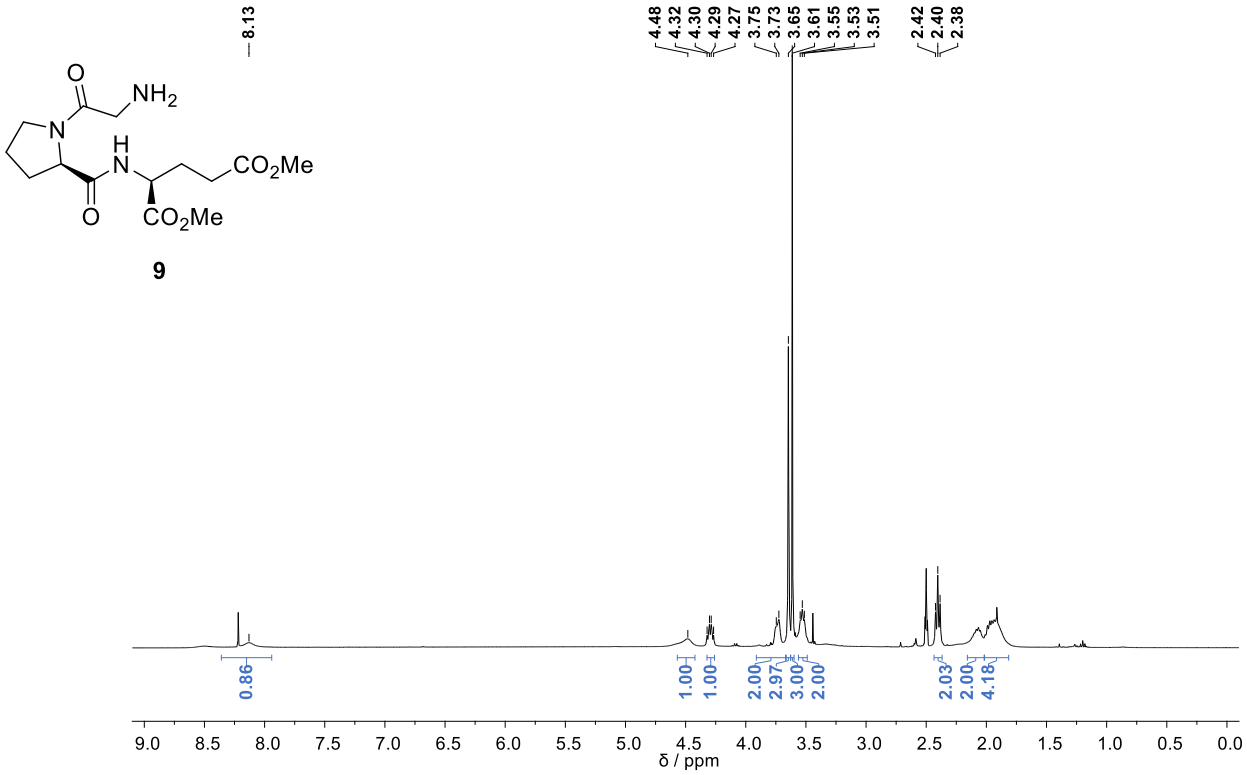

9

Figure S18. ^{1}H-NMR spectrum (400 MHz, DMSO-d_6, 110 ºC) of compound **9**.

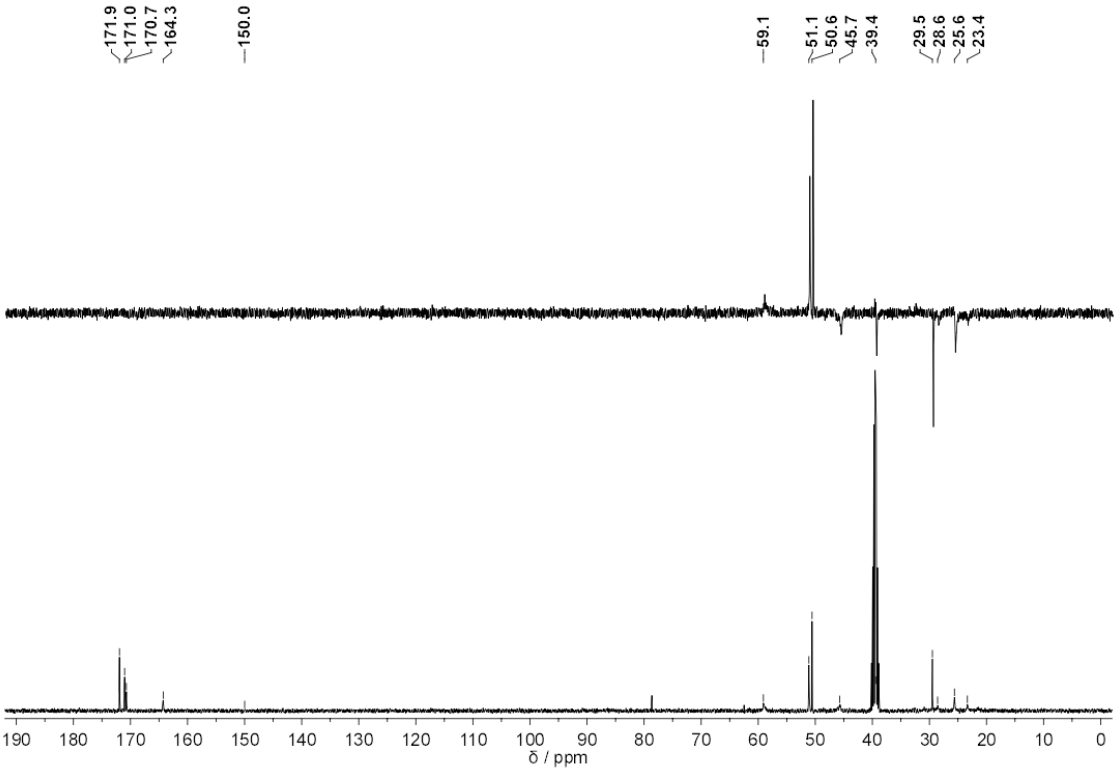

Figure S19. ^{13}C-NMR and DEPT-135 spectra (100 MHz, DMSO-d_6, 110 ºC) of compound **9**.

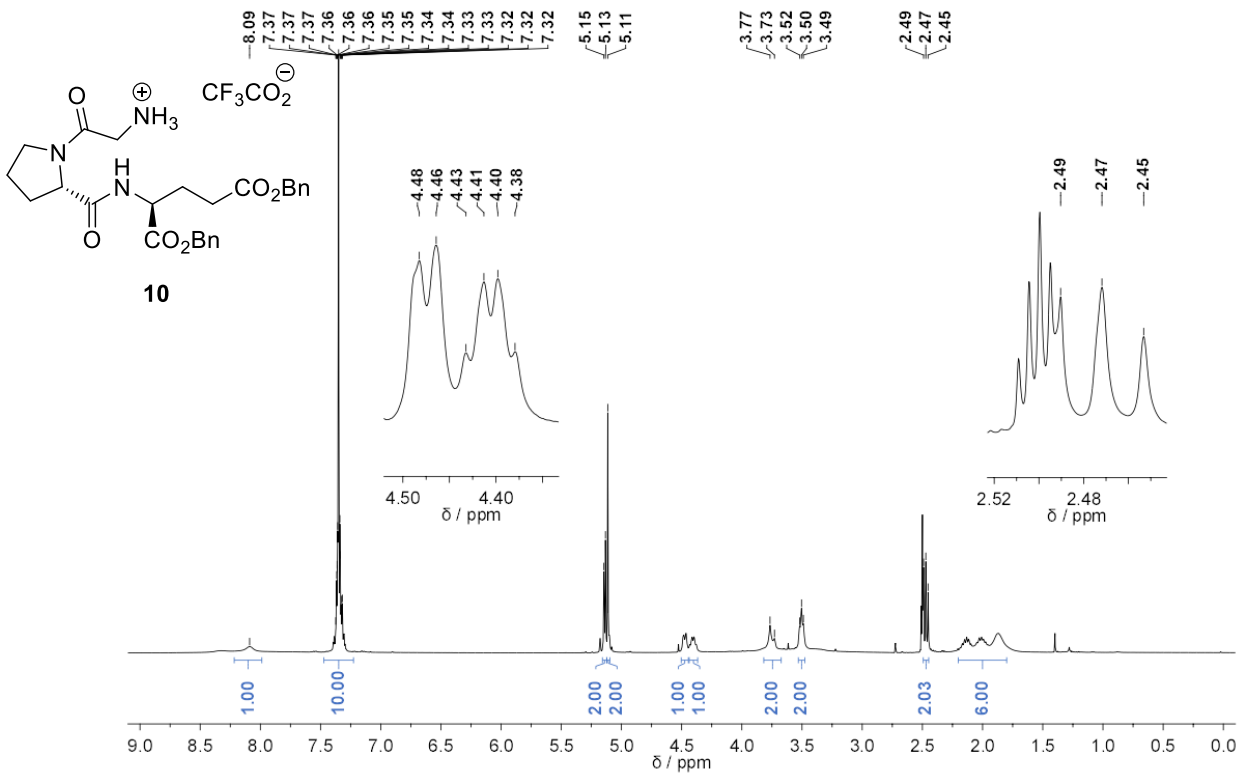

Figure S20. ^{1}H-NMR spectrum (400 MHz, DMSO-d_6, 110 ºC) of compound **10**.

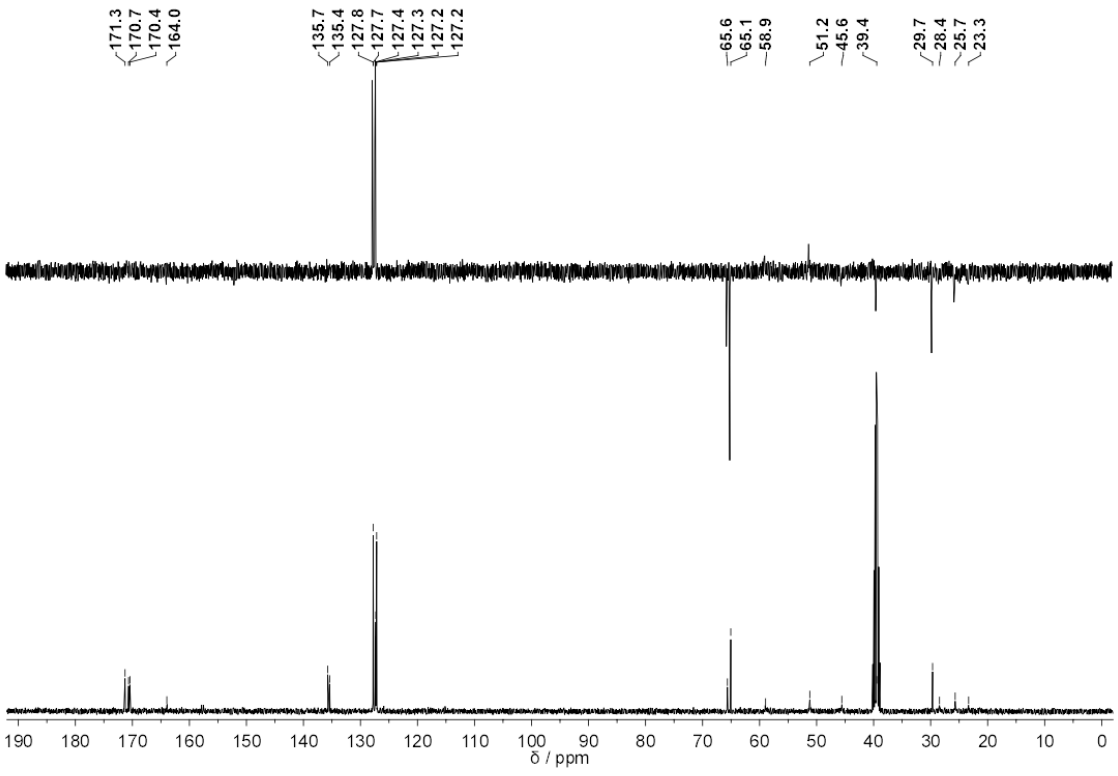

Figure S21. ^{13}C-NMR and DEPT-135 spectra (100 MHz, DMSO-d_6, 110 ºC) of compound **10**.

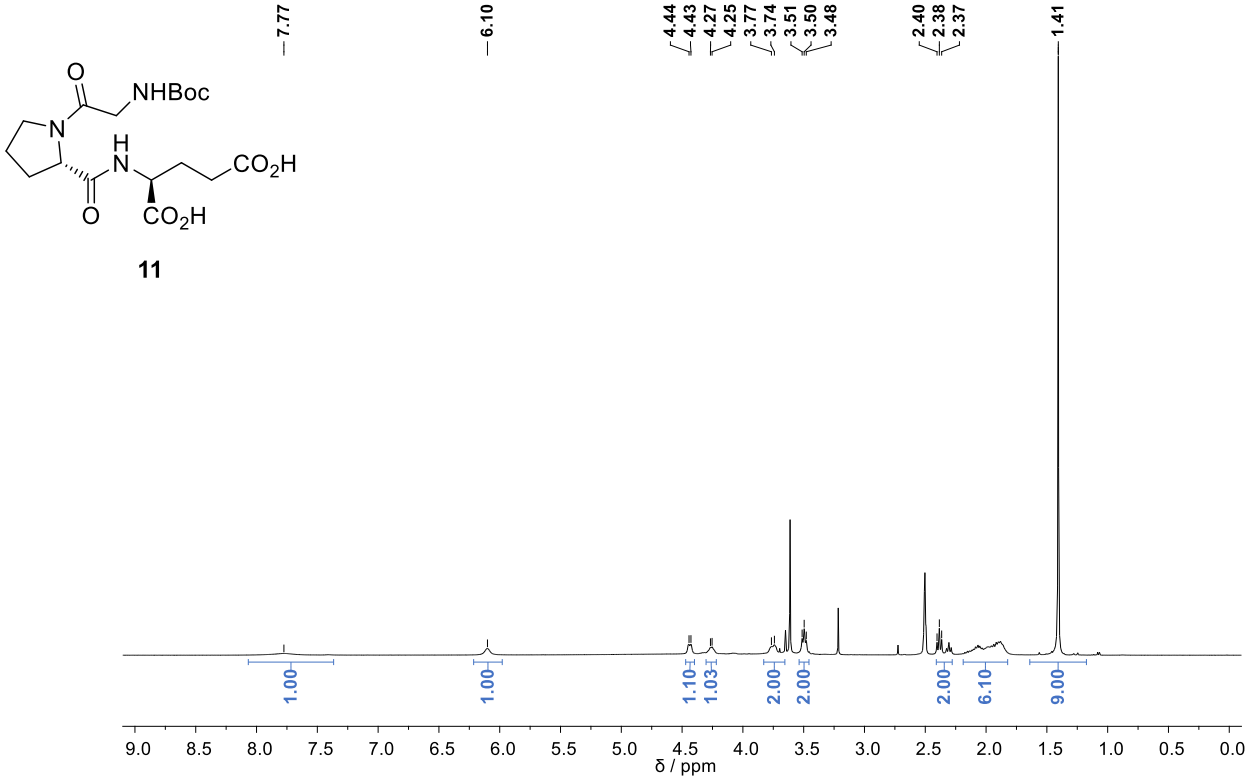

Figure S22. ^{1}H-NMR spectrum (400 MHz, DMSO-d_6, 110 ºC) of compound **11**.

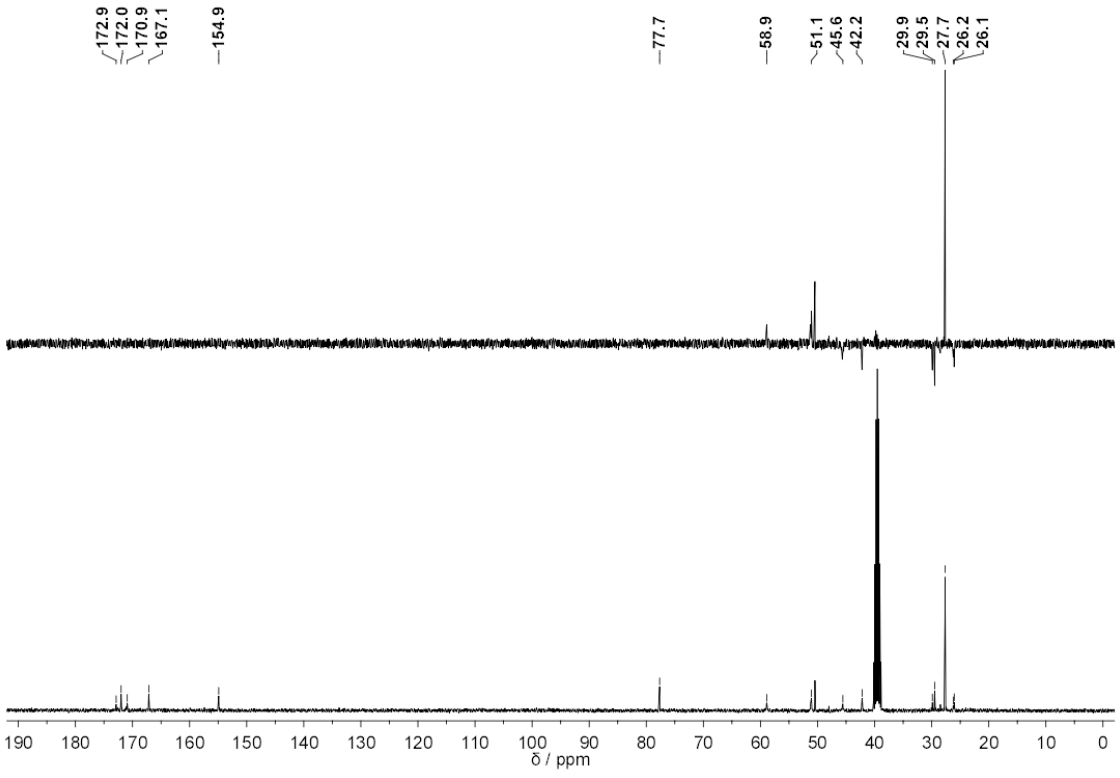

Figure S23. ^{13}C-NMR and DEPT-135 spectra (100 MHz, DMSO-d_6, 110 ºC) of compound **11**.

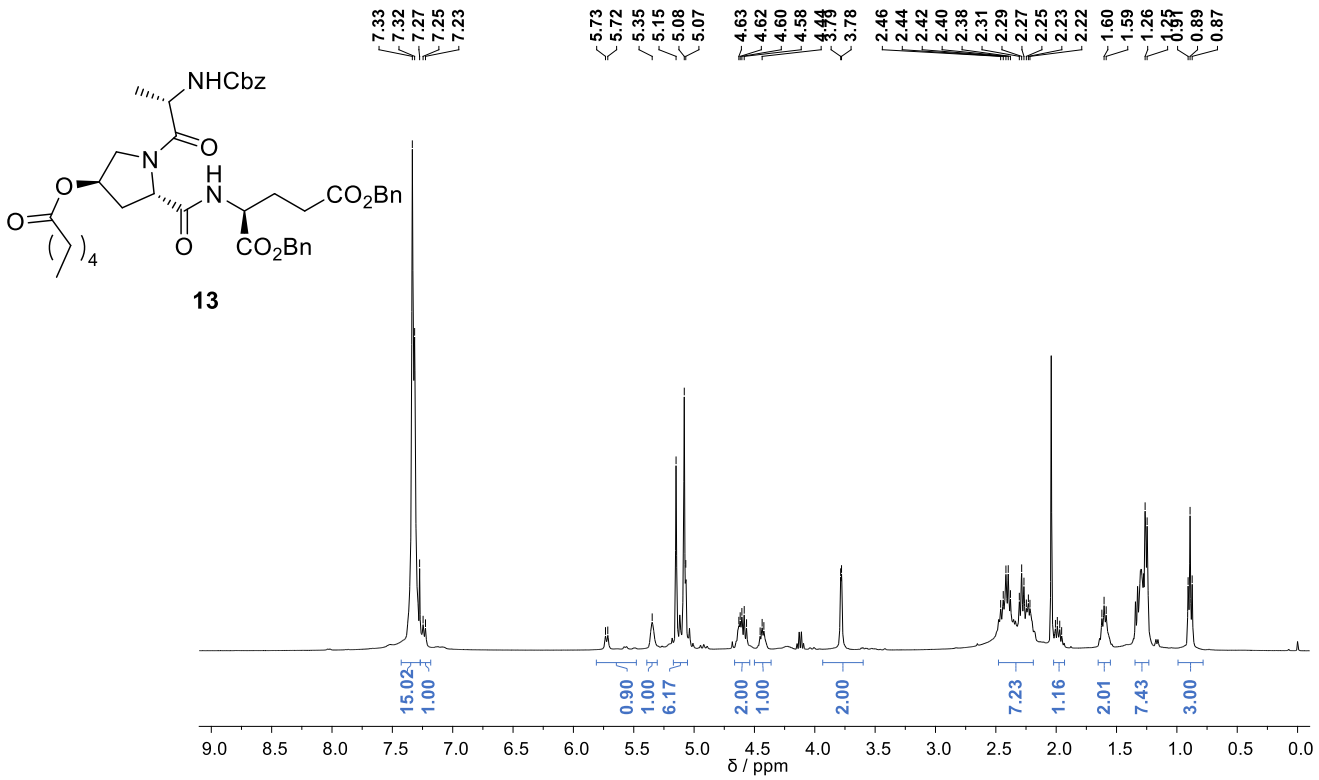

Figure S24. ^{1}H-NMR spectrum (400 MHz, $CDCl_3$, 26 ºC) of compound **13**.

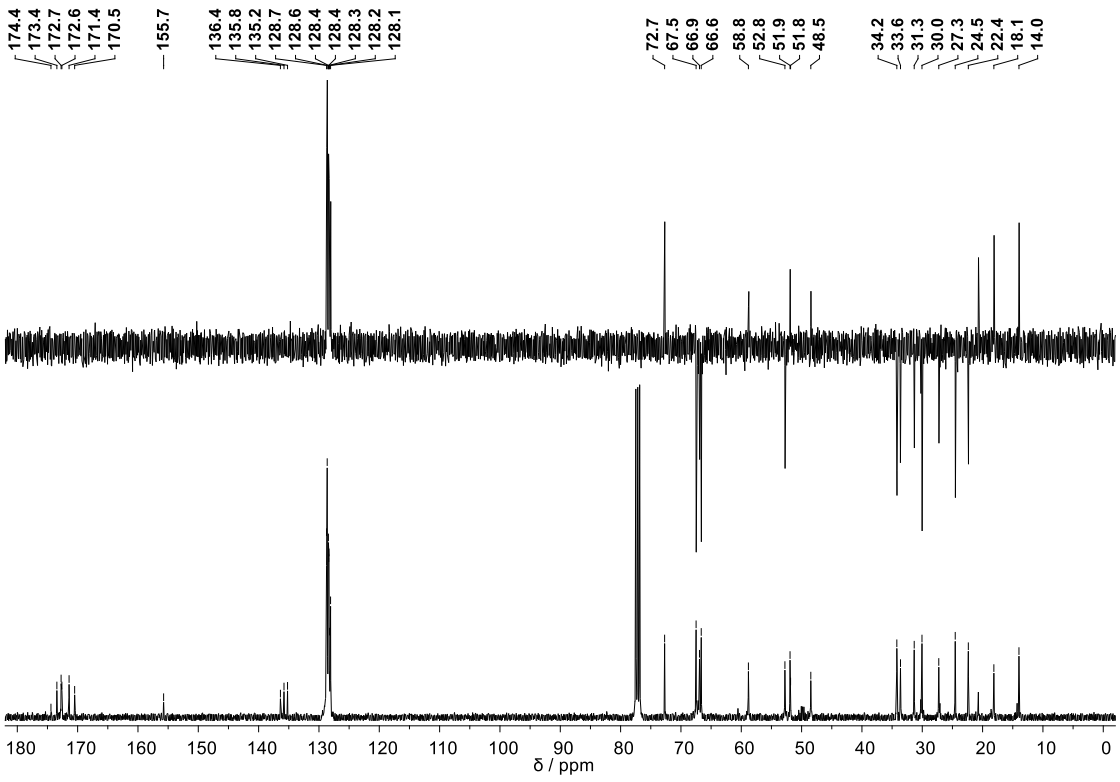

Figure S25. ^{13}C-NMR and DEPT-135 spectra (100 MHz, $CDCl_3$, 26 ºC) of compound **13**.

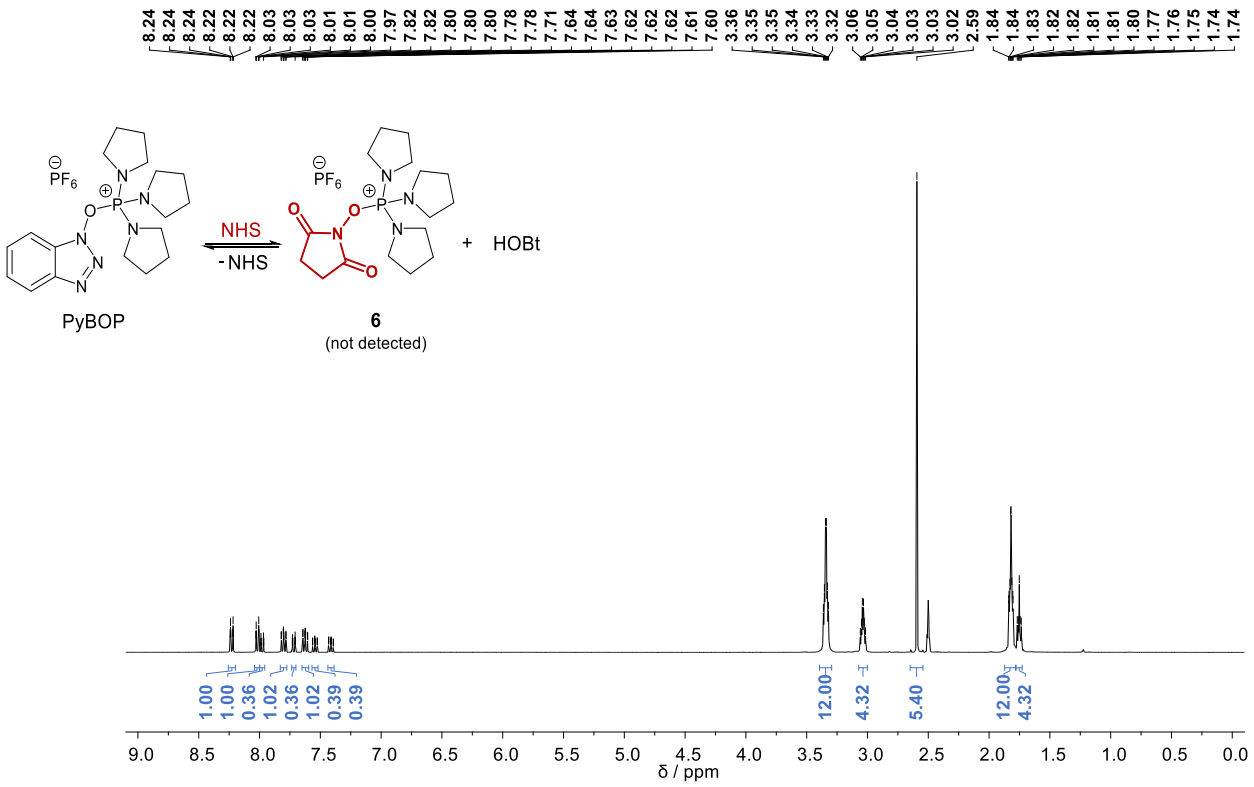

Figure S26. ^{1}H-NMR spectrum (400 MHz, DMSO-d_6, 26 ºC) of PyBOP-NHS interaction.

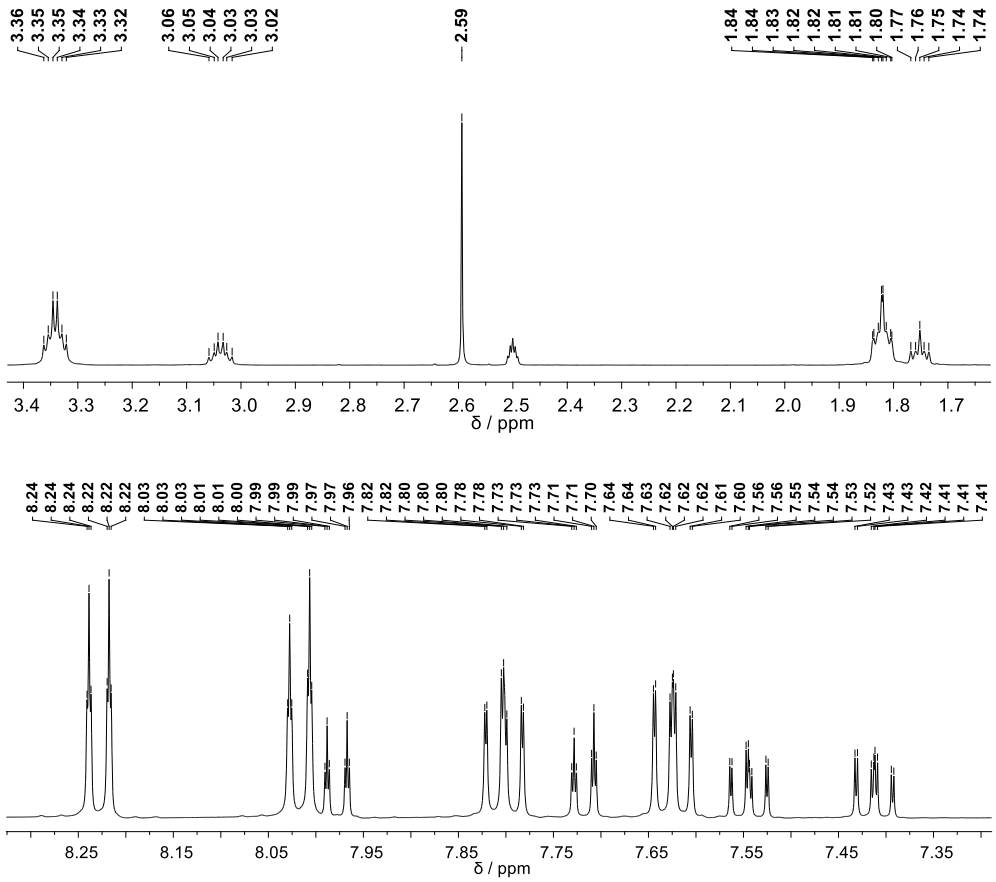

Figure S27. ^{1}H-NMR spectrum (400 MHz, DMSO-d_6, 26 ºC) expansions of PYBOP-NHS interaction.

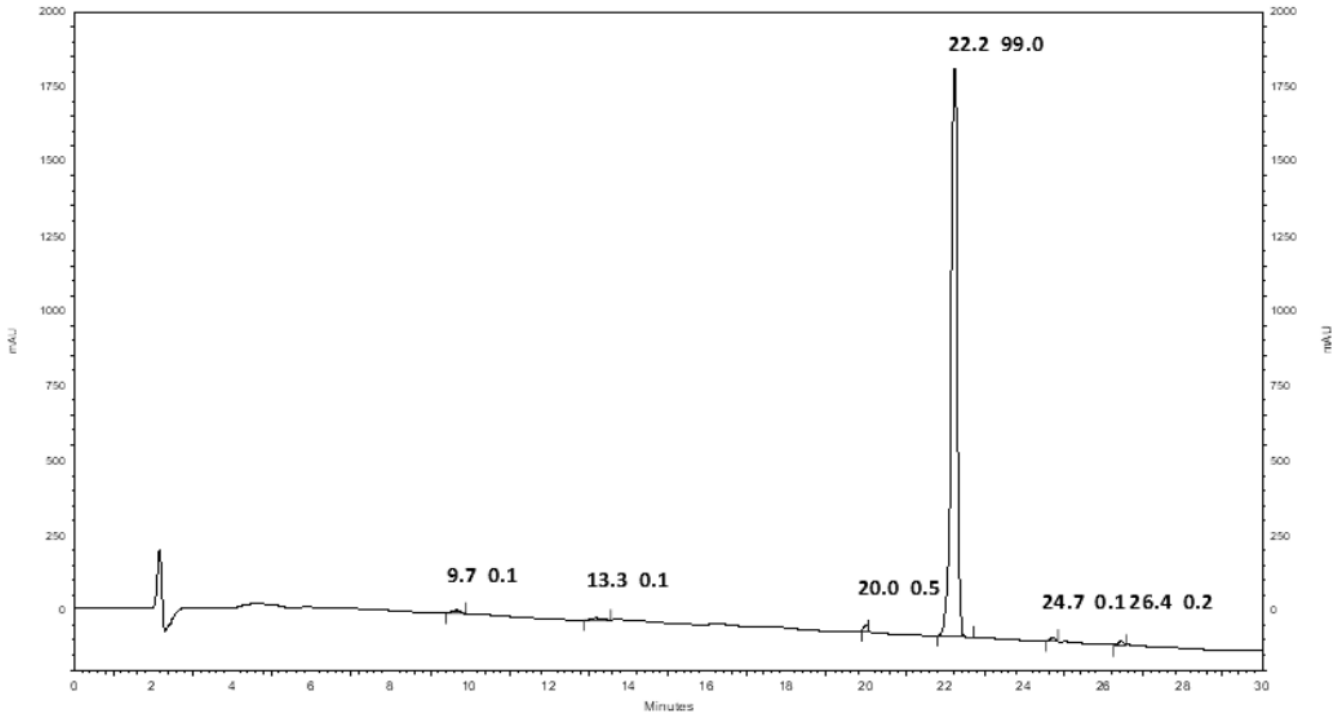

Figure S28. rp-HPLC chromatogram of tripeptide **5**.

VT-NMR and *in silico* study for the *cis-trans* isomerization of tripeptide 5

Cis-trans isomerization is commonly observed phenomenon in which rotation about a single bond is hindered by a rotational energy barrier, therefore leading to the presence of different conformers in solution.[1] In proline-containing peptides conformers are usually associated to the *cis-trans* peptide bond isomerization at proline residue (X-Pro), with different population distribution depending on the temperature and solvent used, being the *cis*-conformer in general the less populated form.[2] The occurrence of the *cis* conformers in X-Pro peptide bonds comes from the fact that this conformation is only about 0.5 kcal mol^{-1} less stable than the *trans* conformer.[3] This two distinct conformations in X-Pro peptides can be defined by the torsion angle ω, defined as the angle made from C_α-C-N-C_α, with ω = 0° for *cis* and ω = ± 180° for *trans*. The *cis-trans* isomerization phenomena in many prolyl-containing peptides and proteins is responsible for a large conformational repertoire, which may be involved in the modulation the protein's activity in many biological processes such as neurodegeneration,[4] cell signaling,[5] among others,[6] with retention of the absolute configuration.[7]

Conformers can be easily distinguished from epimers using variable-temperature NMR (VT-NMR) experiments.[8] In presence of rotamers, VT-NMR should denote the coalescence of the signals as the temperature rises,[8] which does not occur when dealing with epimers. The VT-NMR experiments (^{1}H-NMR in DMSO-d_6) show the coalescence of signals as temperature increases from 26 ºC to 110 ºC (**Figure S29**). After recording the sample at 110 ºC, a new spectrum at 26 ºC was recorded. Both spectra taken at 26 ºC were superimposable, indicating there was no degradation during the study.

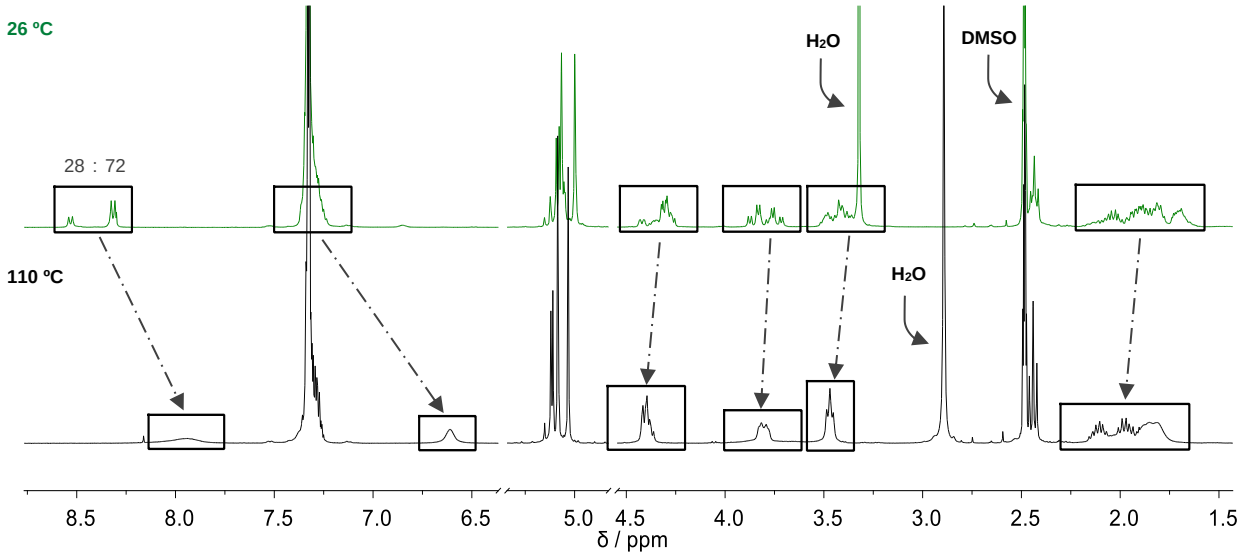

Figure S29. Stacked ^{1}H-NMR spectra of tripeptide **5** (400 MHz, DMSO-d_6) at 26 ºC and 110 ºC.

These data endorse stereochemical integrity of tripeptide **5**, by demonstrating that the origin of the splitting pattern found in the NMR spectra at 26 ºC results from *cis-trans* phenomena and not from epimerization events. It was found that tripeptide **5** exists as a 72:28 mixture of conformers at rt (DMSO-d_6), determined by integration of glutamate amide proton (8.3-8.6 ppm), which was unambiguously attributed by TOCSY analysis (see **Figure S3** for details). It is well-known that *cis*-conformers are generally favoured in solvents with a large dipolar moment such as DMSO (3.96 D).[9] Therefore, in order to correctly assign the *major* and *minor* conformers (in DMSO-d_6 at rt) it was performed a ROESY experiment (**Figure S30**). By analysis of ROESY spectrum it was observed that the *major* conformer (NH_{Glu}) species has crosspeaks with the α-protons of Gly, while in the *minor* conformer these crosspeaks are absent (**Figure S30**). This suggests that *cis*-**5** s is the most populated specie in DMSO-d_6 at rt.

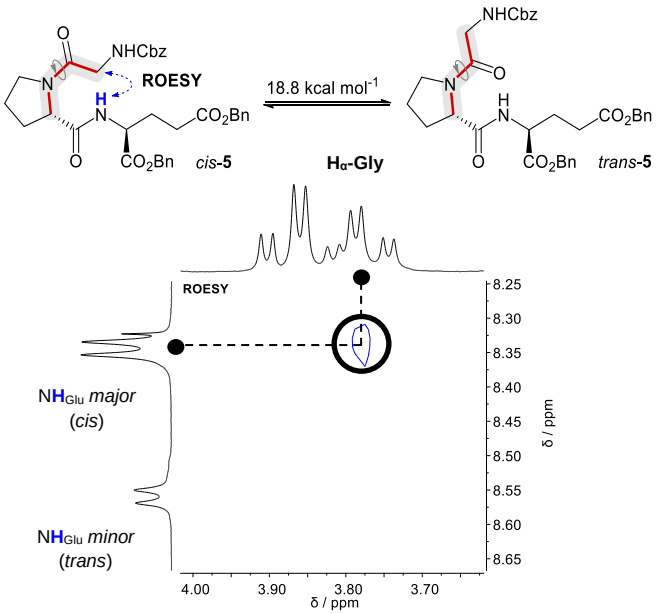

Figure S30. Selected crosspeaks from ROESY experiment (DMSO-d_6, 26 ºC) of tripeptide **5**.

The free energy barriers associated to *cis-trans* isomerization about the torsion angle ω are relatively high (~20 kcal mol^{-1}),[10] albeit it is known that both energy barriers and the population distribution may be influenced by chemical substitutions and side chain effects.[11]

The free energy of activation for the *cis-trans* isomerization of tripeptide **5** was calculated using Eyring's equations (**a** and **b**) as modified by Shanan-Atidi and Bar-Eli.[12]

$$\Delta G_{\mathrm{A}}^{\ddagger} = 4.57\, T_c \left[10.62 + \log\frac{X}{2\pi(1-\Delta P)} + \log\frac{T_c}{\delta_\nu}\right]$$

$$\Delta G_{\mathrm{B}}^{\ddagger} = 4.57\, T_c \left[10.62 + \log\frac{X}{2\pi(1+\Delta P)} + \log\frac{T_c}{\delta_\nu}\right]$$

where $X = 2\pi\tau\Delta_\nu$ and $\Delta P = P_A - P_B$.

P_A and P_B represent the population of the conformers A and B ($P_A > P_B$, $P_A + P_B = 1$), respectively, and τ is the mean lifetime. T_c and $\Delta\nu$ are the coalescence temperature and the chemical shift difference between conformers A and B, respectively. X is obtained using equation (**c**):

$$P_A - P_B = \Delta P = \frac{1}{X}\sqrt{\left(\frac{X^2-2}{3}\right)^3}$$

From the ^{1}H-NMR spectrum at 299 K, the frequency difference, $\Delta\nu$, between the amide signals was 85.99 Hz (85.99 s^{-1}). The Coalescence Temperature, T_c, was 383 K.

$$\Delta P = \frac{0.72-0.28}{1} = \frac{1}{X}\sqrt{\left(\frac{X^2-2}{3}\right)^3} \Leftrightarrow X = 1.715$$

$$\Delta G_{\mathrm{A}}^{\ddagger} = 4.57\,(383)\left[10.62 + \log\frac{1.715}{2\pi(1-0.1024)} + \log\frac{383}{85.99}\right] = 18.8\ \mathrm{kcal\ mol^{-1}}$$

$$\Delta G_{\mathrm{B}}^{\ddagger} = 4.57\,(383)\left[10.62 + \log\frac{1.715}{2\pi(1+0.1024)} + \log\frac{383}{85.99}\right] = 18.7\ \mathrm{kcal\ mol^{-1}}$$

The experimental data show an energy barrier of 18.8 kcal mol^{-1}, which clarifies the splitting signal pattern found in the ^{1}H- and ^{13}C-NMR spectra at 26 ºC.

***In silico* experiments**

To get more insights about the origin of the *cis-trans* isomerization of **5**, *in silico* experiments were performed. The geometries of the *cis* and *trans* conformers of tripeptide **5** were optimized using the Gaussian 09 software package[13] at the M06-2X/6-31G(d,p) level of theory,[14] in implicit DMSO (**Figure S31**). The energies were latter re-evaluated at the M06-2X/6-311+G(d,p) level of theory. Implicit solvation was considered with the SMD model, which is based on the integral equation formalism model (IEFPCM) but with radii and nonelectrostatic terms of Truhlar and co-workers' SMD solvation model. SMD has the advantage of including nonelectrostatic terms in the calculations.[15] The M06-2X density functional was used due to good results in applications involving main-group thermochemistry, kinetics and noncovalent interaction.[14, 16]

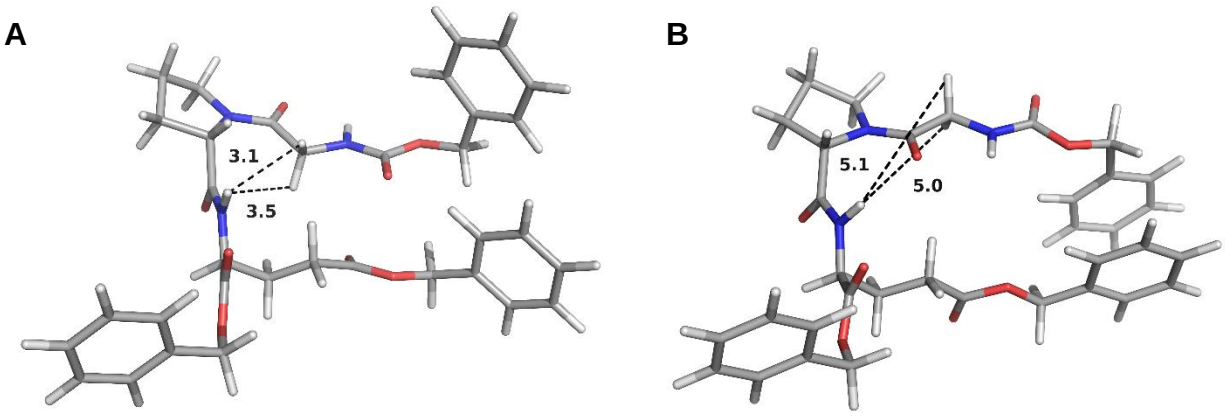

Figure S31. Optimized geometries, at the M06-2X/6-31(d,p) level of theory, for the *cis* (**A**) and *trans* (**B**) species of tripeptide **5**.

As can be observed from **Figure S31**, both *cis* and *trans* conformational isomers have similar puckering modes, with the π-stacking between two benzyl groups being of note (one from the Cbz protecting group of Gly residue and the other from the benzyl ester of Glu residue side chain).

The major difference relies on the torsion angle ω associated with the proline *cis-trans* isomerization. More specifically, it was found ω = −1.1º for the *cis* species and ω = −175.6º for the *trans* counterpart. The torsion angle in *cis*-**5** place the α-protons of Gly residue 3.1 and 3.5 Å away from the amide proton of glutamate residue, NH_{Glu}, while the same atoms in *trans*-**5** are separated by 5.0 and 5.1 Å. This observation helps to explain why crosspeaks between the α-protons of Gly and NH_{Glu} were only possible to detect for the *major* rotamer, assigned as the *cis* conformer (*cis*-**5**), which agrees with the spectroscopic data obtained.

The energy difference between the species was calculated at the at the M06-2X/6-31G(d,p) level of theory in implicit DMSO, and consisted in the electronic energy plus zero-point correction. It was found that *cis*-**5** is slightly more stable, by 0.6 kcal mol^{-1}, than the *trans* counterpart. Given this, it is possible to identify the *cis* species as the dominant rotamer at room temperature. Moreover, this small energy difference helps to justify why both species are present in an appreciable ratio at room temperature.

The *cis–trans* proline isomerization was subsequently modelled by constructing a potential energy curve (**Figure S32**).

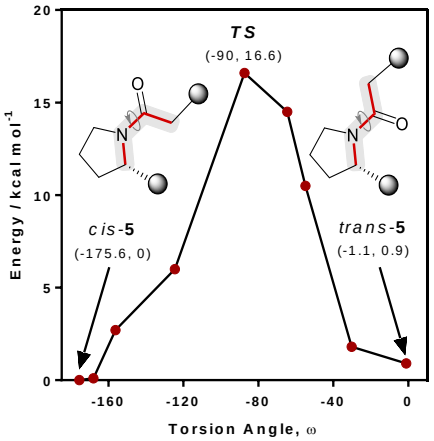

Figure S32. Potential energy curve of the *cis–trans* isomerization of tripeptide **5**, as a function of the torsion angle (ω) at proline residue. Calculations were made at the M06-2X/6-311+G(d,p)//M06-2X/6-31G(d,p) level of theory, in implicit DMSO.

This was done by optimizing the geometry of tripeptide **5** at several torsion angles, which were fixed during the geometry optimizations at the M06-2X/6-31G(d,p) level of theory in implicit DMSO, while the energies were re-evaluated at the M06-2X/6-311+G(d,p) level of theory. The calculations identified once again the *cis* species as the most stable one, this time by 0.9 kcal mol^{-1}.

Interestingly, these calculations revealed an energy barrier of 16.6 kcal mol^{-1} (**Figure S32**), with an energy maximum corresponding to the structure with ω = −90.0º. Such barrier is quite similar (~2 kcal mol^{-1} lower) to the activation energy determined experimentally, which strengthen the hypothesis that the signal duplication pattern found at room temperature in the NMR spectra may be related to the *cis–trans* isomerization at proline residue.

Thermal shift coefficient NMR investigation: the nature of the hydrogen bonding interaction

The nature of intramolecular hydrogen bonds in peptides can be studied by the analysis of the thermal behaviour of hydrogen bonds using NMR, which is considered an appropriate and elegant tool to study the exact nature of these interactions.[9] This approach is based on the fact that intramolecular hydrogen bonding between a hydrogen bond donor (amide proton) and an acceptor (carbonyl oxygen) is disturbed with the increase of the temperature. Using aprotic solvents, such as DMSO-d_6, the amide proton signals in ^{1}H-NMR spectra experience a downfield shift (less through space deshielding).[9] By plotting the chemical shift (δ, in ppb) as a function of temperature (in kelvin), the thermal shift coefficient is given by $-\Delta\delta/\Delta T$.

When $-\Delta\delta/\Delta T$ > 5 ppb K^{-1}, intramolecular hydrogen bonding is absent and the amide protons are solvent-exposed.[9] The plott $-\Delta\delta/\Delta T$ for NH_{Glu} amide protons in both conformers of tripeptide **5** is shown in **Figure S33**. It was found $-\Delta\delta/\Delta T$ = 4.421 ± 0.074 (R^2 = 0.9994) for *trans*-conformer and $-\Delta\delta/\Delta T$ = 5.139 ± 0.013 (R^2 = 1) for *cis*-conterpart.

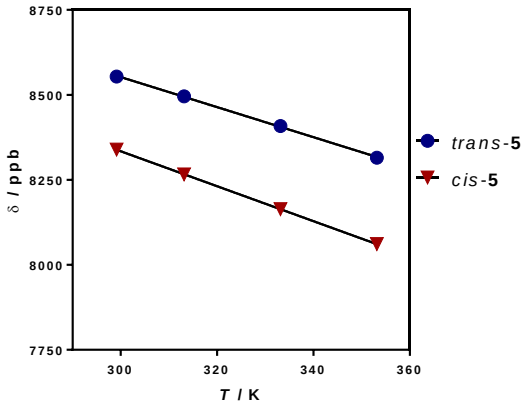

Figure S33. The hydrogen bond investigation with thermal coefficient plots for NH_{Glu} present in *cis*-*trans* conformers of tripeptide **5** (solvent: DMSO-d_6, temperature: 299-353 K).

This result shows that NH_{Glu} in *cis*-conformer does not participate in intramolecular H-bonding,[9] which agrees with the optimized geometry for this conformer as depicted in **Figure 31A**.

Therefore, the theoretical calculations together with the NMR data for perbenzylated tripeptide **5** are consistent with the hypothesis that the two rotamers of **5** are originated from a high energy barrier associated with the rotation about the tertiary amide bond at the proline residue.

E-factor calculation (Tripeptide 5)

$$\mathbf{E-factor} = \text{Kg (waste)/ Kg (product)}$$

Classical Iterative Synthesis:

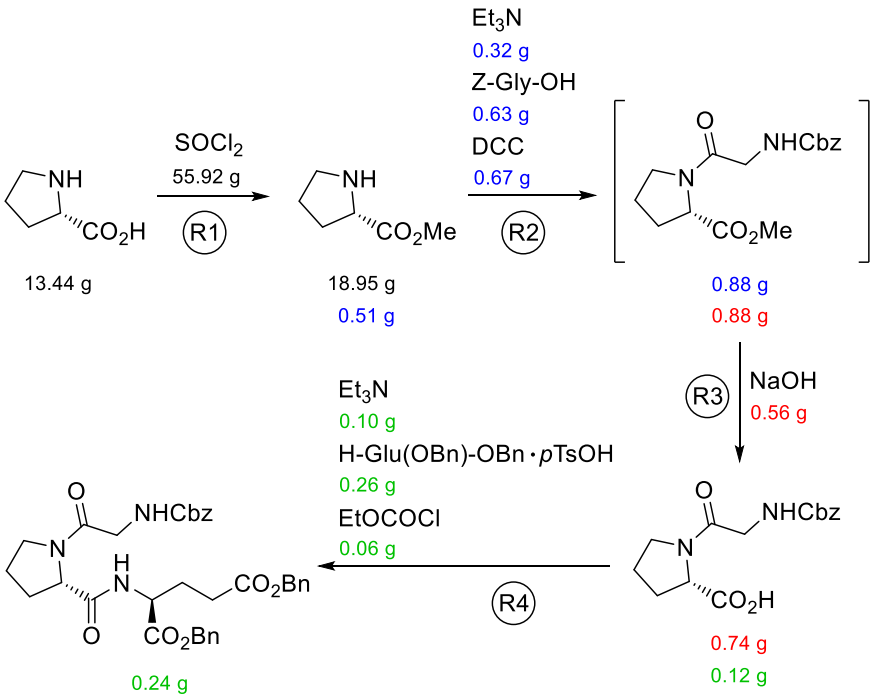

$$\text{R1} = \frac{13.44\ \text{g} + 55.92\ \text{g} - 18.95\ \text{g}}{18.95\ \text{g}} = 2.66$$

$$\text{R2} = \frac{0.51\ \text{g} + 0.32\ \text{g} + 0.63\ \text{g} + 0.67\ \text{g} - 0.88\ \text{g}}{0.88\ \text{g}} = 1.42$$

$$\text{R3} = \frac{0.88\ \text{g} + 0.56\ \text{g} - 0.74\ \text{g}}{0.74\ \text{g}} = 0.95$$

$$\text{R4} = \frac{0.12\ \text{g} + 0.10\ \text{g} + 0.26\ \text{g} + 0.06\ \text{g} - 0.24\ \text{g}}{0.24\ \text{g}} = 1.25$$

$$\mathbf{E-factor} = \text{R1} + \text{R2} + \text{R3} + \text{R4} = 6.3$$

One-pot Process:

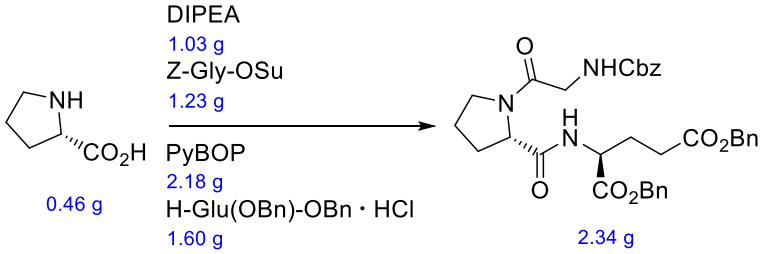

$$\mathbf{E-factor} = \frac{0.46\ \mathrm{g} + 1.03\ \mathrm{g} + 1.23\ \mathrm{g} + 2.18\ \mathrm{g} + 1.60\ \mathrm{g} - 2.34\ \mathrm{g}}{2.34\ \mathrm{g}} = 1.8$$

Table S1. Cartesian coordinates of *cis*-**5**, obtained at the M06-2X/6-31G(d,p) level of theory in implicit DMSO. Energy = −2083.297685 hartrees.

Atom	x	y	z	Atom	x	y	z
C	-1.23150	7.48520	-1.60020	C	10.70500	3.96720	-2.61380
C	-2.41110	6.92560	-1.11430	C	11.01260	4.83930	-3.65780
C	-2.40240	6.21730	0.08720	C	11.69280	6.02760	-3.40450
C	-1.21620	6.07310	0.80060	C	12.06750	6.34280	-2.09850
C	-0.02880	6.62890	0.31590	C	11.75860	5.47350	-1.05630
C	-0.04290	7.33190	-0.88920	H	4.49880	2.35110	-3.47710
C	1.25120	6.44960	1.08870	H	-1.23540	8.03810	-2.53450
O	1.71690	5.08080	1.02240	H	-3.33760	7.04230	-1.66830
C	2.34330	4.72650	-0.09760	H	-3.32130	5.78420	0.47030
C	2.80850	3.28400	-0.02910	H	-1.20820	5.52750	1.74100
O	2.55620	5.46450	-1.03260	H	0.88290	7.75310	-1.27020
N	3.31620	2.92180	-1.33400	H	1.09750	6.62530	2.15430
H	1.95060	2.65050	0.21940	H	2.03670	7.11200	0.71910
C	3.88170	3.11590	1.06020	H	3.50230	3.66650	-1.99520
C	5.06940	4.04800	0.84870	H	4.21410	2.07530	1.03100
C	6.27510	3.61450	1.64290	H	3.42660	3.29130	2.03910
O	6.56600	2.46500	1.89050	H	4.82750	5.08530	1.09780
O	6.99690	4.66630	2.04280	H	5.39340	4.03090	-0.20100
C	8.25000	4.37070	2.67590	H	8.72660	3.54980	2.13050
C	9.08460	5.62130	2.64040	H	8.07040	4.04080	3.70390
C	9.32600	6.25730	1.41720	H	8.90860	5.82750	0.50860
C	10.09690	7.41540	1.37050	H	10.27960	7.90310	0.41700
C	10.64140	7.94280	2.54240	H	11.24310	8.84580	2.50560
C	10.41010	7.30780	3.76000	H	10.82950	7.71460	4.67510
C	9.62980	6.15280	3.80850	H	9.44030	5.66330	4.76030
C	3.56130	1.63520	-1.65320	H	2.44130	1.63740	-4.48480
O	3.35210	0.69830	-0.89270	H	2.28280	0.28100	-3.34770
C	4.09840	1.41580	-3.06720	H	4.22830	0.44730	-5.70160
C	2.98550	0.84470	-3.96980	H	3.06850	-0.85280	-5.35820
C	3.72820	-0.11130	-4.90440	H	5.66390	-1.09300	-4.49860
C	4.76810	-0.74210	-3.98400	H	4.34700	-1.57450	-3.40750
N	5.11510	0.36630	-3.08900	H	5.92080	1.55900	-0.63480
C	6.27120	0.36630	-2.39930	H	6.33810	2.51530	-2.06860
O	7.07500	-0.56210	-2.45820	H	8.43820	0.66430	-1.34680
C	6.56170	1.58840	-1.52790	H	11.70180	2.88670	0.20470
N	7.95530	1.53710	-1.17150	H	10.36100	3.93910	0.68620
C	8.62030	2.60210	-0.69410	H	10.17720	3.04040	-2.82150
O	8.14370	3.70710	-0.48600	H	10.71930	4.58660	-4.67230
O	9.92010	2.28200	-0.48310	H	11.92940	6.70490	-4.21920
C	10.78230	3.36410	-0.14340	H	12.59740	7.26770	-1.89080
C	11.07410	4.28130	-1.30650	H	12.04560	5.72000	-0.03650

Table S2. Cartesian coordinates of *trans*-**5**, obtained at the M06-2X/6-31G(d,p) level of theory in implicit DMSO. Energy = −2083.295124 hartrees.

Atom	x	y	z	Atom	x	y	z
C	-2.16110	-1.37690	2.74670	C	10.38120	-0.56700	-0.62090
C	-3.05990	-2.31520	2.24390	C	11.17670	-1.69360	-0.82970
C	-2.60830	-3.58150	1.87240	C	12.53280	-1.66570	-0.51540
C	-1.26220	-3.90760	2.00840	C	13.09420	-0.50080	0.00750
C	-0.35560	-2.96910	2.50940	C	12.30180	0.62580	0.20600
C	-0.81200	-1.70210	2.87290	H	2.42310	0.42570	-2.93750
C	1.10030	-3.33100	2.64200	H	-2.50870	-0.39000	3.03630
O	1.70850	-3.55150	1.34900	H	-4.11080	-2.06210	2.14220
C	1.99870	-2.45630	0.64570	H	-3.30680	-4.31510	1.48180
C	2.65500	-2.81440	-0.67580	H	-0.90930	-4.89610	1.72480
O	1.81030	-1.32500	1.02920	H	-0.10410	-0.96950	3.25030
N	2.68560	-1.62290	-1.49260	H	1.22560	-4.28360	3.15910
H	2.04150	-3.56770	-1.17930	H	1.65460	-2.55300	3.17110
C	4.05360	-3.40960	-0.43030	H	2.78670	-0.72510	-1.03260
C	4.96990	-2.45330	0.32220	H	4.48120	-3.65010	-1.40710
C	6.34420	-3.03800	0.52220	H	3.94910	-4.34740	0.12260
O	6.72360	-4.10440	0.09780	H	4.57530	-2.20470	1.31520
O	7.12250	-2.21940	1.24930	H	5.07920	-1.50150	-0.21430
C	8.44550	-2.69610	1.51000	H	8.94880	-2.90570	0.55920
C	9.21390	-1.66020	2.28660	H	8.38640	-3.63970	2.06370
C	8.66790	-0.43300	2.65560	H	7.63810	-0.20470	2.40490
C	9.44790	0.50250	3.33850	H	9.01300	1.45620	3.62380
C	10.77640	0.22350	3.64490	H	11.38220	0.95700	4.16820
C	11.32580	-1.00610	3.27530	H	12.36290	-1.23150	3.50590
C	10.54780	-1.94140	2.60370	H	10.97890	-2.89460	2.30490
C	2.88910	-1.68870	-2.82440	H	1.45500	-0.05950	-5.07760
O	2.99330	-2.74570	-3.43580	H	2.55660	-1.43050	-5.31480
C	2.96880	-0.31980	-3.52540	H	3.22400	1.53710	-5.66400
C	2.48960	-0.39180	-4.98130	H	3.52900	0.22240	-6.81820
C	3.48170	0.47780	-5.75800	H	5.52950	1.01200	-5.16850
C	4.80120	0.21050	-5.03900	H	5.24960	-0.73490	-5.36560
N	4.37410	0.10710	-3.63720	H	6.39470	2.02380	-3.35060
C	5.03390	0.56520	-2.56130	H	7.01420	0.36960	-3.40470
O	4.53650	0.57980	-1.43060	H	6.51100	1.08060	-0.68140
C	6.44730	1.07960	-2.79220	H	10.20840	2.16790	1.16940
N	7.06910	1.26000	-1.50680	H	10.50090	2.67010	-0.50850
C	8.35910	1.63480	-1.40540	H	9.31780	-0.61650	-0.84090
O	9.09060	1.89630	-2.34210	H	10.73130	-2.59740	-1.23590
O	8.73670	1.67080	-0.10400	H	13.14890	-2.54510	-0.67640
C	10.12930	1.85860	0.12440	H	14.14970	-0.46980	0.26040
C	10.93980	0.60390	-0.10900	H	12.74100	1.53400	0.61320

References:

[1] V. M. Potapov, Mir Publishers: Moscow, Russia, 1978, pp. 27-28.

[2] A. E. Aliev, S. Bhandal, D. Courtier-Murias, *J. Phys. Chem. A,* 2009, **113**, 10858-10865.

[3] K. Kim, J. P. Dumas Jp, J. P. Germanas, *J. Org. Chem.*, 1996, **61**, 3138-3144.

[4] L. Pastorino, A. Sun, P. J. Lu, X. Z. Zhou, M. Balastik, G. Finn, G. Wulf, J. Lim, S. H. Li, X. Li, W. Xia, L. K. Nicholson, K. P. Lu, *Nature*, 2006, **440**, 528-534.

[5] a) P. Sarkar, T. Saleh, S. R. Tzeng, R. B. Birge, C. G. Kalodimos, *Nat. Chem. Biol.*, 2011, **7**, 51-57; b) P. Sarkar, C. Reichman, T. Saleh, R. B. Birge, C. G. Kalodimos, *Mol. Cell*, 2007, **25**, 413-426; c) G. Wulf, G. Finn, F. Suizu, K. P. Lu, *Nat. Cell Biol.*, 2005, **7**, 435-441; d) K. N. Brazin, R. J. Mallis, D. B. Fulton, A. H. Andreotti, *Proc. Natl. Acad. Sci. U.S.A.*, 2002, **99**, 1899-1904.

[6] a) I. M. Paulsen, I. L. Martin, S. M. Dunn, *J. Neurochem.*, 2009, **110**, 870-878; b) C. J. Nelson, H. Santos-Rosa, T. Kouzarides, *Cell*, 2006, **126**, 905-916; c) K. E. Fathers, E. S. Bell, C. V. Rajadurai, S. Cory, H. Zhao, A. Mourskaia, D. Zuo, J. Madore, A. Monast, A. M. Mes-Masson, A. A. Grosset, L. Gaboury, M. Hallet, P. Siegel, M. Park, *Breast Cancer Res.* 2012, **14**, R74; d) H. Yanagi, L. Wang, H. Nishihara, T. Kimura, M. Tanino, T. Yanagi, S. Fukuda, S. Tanaka, *Biochem. Biophys. Res. Commun.*, 2012, **418**, 104-109; e) Y. Dai, L. Qi, X. Zhang, Y. Li, M. Chen, X. Zu, *Cell Biochem. Funct.*, 2011, **29**, 625-629; f) J. Wang, Y. L. Che, G. Li, B. Liu, T. M. Shen, H. Wang, H. Linghu, *Mol. Carcinog.*, 2011, **50**, 506-515; g) C. T. Miller, G. Chen, T. G. Gharib, H. Wang, D. G. Thomas, D. E. Misek, T. J. Giordano, J. Yee, M. B. Orringer, S. M. Hanash, D. G. Beer, *Oncogene*, 2003, **22**, 7950-7957.

[7] a) C. Dugave, L. Demange, *Chem. Rev.*, 2003, **103**, 2475-2532; b) K. P. Lu, G. Finn, T. H. Lee, L. K. Nicholson, *Nat. Chem. Biol.*, 2007, **3**, 619-629; c) W. J. Wedemeyer, E. Welker, H. A. Scheraga, *Biochemistry*, 2002, **41**, 14637-14644; d) A. H. Andreotti, *Biochemistry*, 2003, **42**, 9515-9524.

[8] I. E. Sampaio-Dias, C. A. D. Sousa, S. C. Silva-Reis, S. Ribeiro, X. Garcia-Mera, J. E. Rodriguez-Borges, *Org. Biomol. Chem.*, 2017, **15**, 7533-7542.

[9] M. D. Farahani, B. Honarparvar, F. Albericio, G. E. M. Maguire, T. Govender, P. I. Arvidsson, H. G. Kruger, *Org. Biomol. Chem.*, 2014, **12**, 4479-4490.

[10] J. Xia, R. M. Levy, *J. Phys. Chem. B*, 2014, **118**, 4535-4545.

[11] E. Beausoleil, W. D. Lubell, *J. Am. Chem. Soc.*, 1996, **118**, 12902-12908.

[12] a) H. Shanan-Atidi, K. H. Bar-Eli, *J. Phys. Chem.*, 1970, **74**, 961-963; b) J. H. Frank, Y. L. Powder-George, R. S. Ramsewak, W. F. Reynolds, *Molecules*, 2012, **17**, 7914-7926.

[13] M. J. Frisch, G. W. Trucks, H. B. Schlegel, G. E. Scuseria, M. A. Robb, J. R. Cheeseman, G. Scalmani, V. Barone, B. Mennucci, G. A. Petersson, H. Nakatsuji, M. Caricato, X. Li, H. P. Hratchian, A. F. Izmaylov, J. Bloino, G. Zheng, J. L. Sonnenberg, M. Hada, M. Ehara, K. Toyota, R. Fukuda, J. Hasegawa, M. Ishida, T. Nakajima, Y. Honda, O. Kitao, H. Nakai, T. Vreven, J. A. Montgomery Jr., J. E. Peralta, F. Ogliaro, M. Bearpark, J. J. Heyd, E. Brothers, K. N. Kudin, V. N. Staroverov, R. Kobayashi, J. Normand, K. Raghavachari, A. Rendell, J. C. Burant, S. S. Iyengar, J. Tomasi, M. Cossi, N. Rega, J. M. Millam, M. Klene, J. E. Knox, J. B. Cross, V. Bakken, C. Adamo, J. Jaramillo, R. Gomperts, R. E. Stratmann, O. Yazyev, A. J. Austin, R. Cammi, C. Pomelli, J. W. Ochterski, R. L. Martin, K. Morokuma, V. G. Zakrzewski, G. A. Voth, P. Salvador, J. J. Dannenberg, S. Dapprich, A. D. Daniels, Ö. Farkas, J. B. Foresman, J. V. Ortiz, J. Cioslowski and D. J. Fox, Gaussian 09, Revision D.01, Gaussian, Inc., Wallingford CT, 2013.

[14] Y. Zhao, D. G. Truhlar, *Theor. Chem. Acc.*, 2008, **120**, 215-241.

[15] A. V. Marenich, C. J. Cramer, D. G. Truhlar, *J. Phys. Chem. B*, 2009, **113**, 6378-6396.

[16] Y. Zhao, D. G. Truhlar, *Acc. Chem. Res.*, 2008, **41**, 157-167.